National Institute of Public Health and Environmental Protection
Bilthoven, the Netherlands

Report nr. 722401005

EDACS: European Deposition maps of Acidifying Components on a Small scale. Model description and preliminary results

W.A.J. van Pul, C.J.M. Potma, E.P. van Leeuwen,
G.P.J. Draaijers, J.W. Erisman

March 1995

This study has been carried out on behalf of and for the account of the Directorate-General of the Environment (DGM/LE) within the Project No 722401: "Air Quality Europe".

Mailing list

1	Directeur Lucht en Energie, ir.G.M.van der Slikke
2	plv.Directeur-Generaal Milieubeheer, dr.ir.B.C.J.Zoeteman
3	Drs.R.J.T.van Lint, DGM, hoofd afd. Luchtkwaliteit en Verzuring
4	Prof.A.Eliassen
5	Dr.E.Berge
6	Dr.H.Sandness
7	Mr.J-P.Tuovinen
8	Dr.P.Grennfelt
9	Dr.P.Borrell
10	Dr.B.Achermann
11	Dr.H.Gregor
12	Dr.R.Guardans
13	Dr.M.Knoflacher
14	Mr.W.Schöpp
15	Dr.S.Dutchak
16	Dr.B.B.Hicks
17	Dr.D.Kallweit
18	Dr.W.Rolle
19	Dr.G.Spindler
20	Dr.C.Baccera
21	Dr.T.Spranger
22	Dr.S.Slanina
23	Dr.B.Wiman
24	Ing.J.H.Duyzer
25	Dr.D. Fowler
26	Ir.P.Hofschreuder
27	Mr.V.G.Keizer
28	Dr.G.Lövblad
29	Mr.H.Marseille
30	Dr.G.van Tol
31	Dr.W.de Vries
32	Dr.G.P.Wyers
33	Dr.F.C.Bosveld
34	Dr.G.W.Heil
35	Ir.A.J.Elshout
36	Ir.W.Ruijgrok

37 Mr.S. Smeulders
38 Depot Nederlandse publicaties en Nederlandse bibliografie
39 Directie RIVM
40 Ir.F. Langeweg
41 Drs.R.J.M. Maas
42 Ir.B.de Haan
43 Drs.J. Bakkes
44 Dr.J.P. Hettelingh
45 Drs.R.J.van de Velde
46 Dr.J.J.M.van Grinsven
47 Dr.D. Onderdelinden
48 Dr.D.van Lith
49 Dr.R.M.van Aalst
50 Drs.E. Buijsman
51 Ing.J.A.van Jaarsveld
52 Dr.L.H.J.M. Janssen
53 Ing.A. Bleeker
54 Drs.J.M.M. Aben
55 Ir.H.S.M.A. Diederen
56-57 Bibliotheek RIVM
58 Bibliotheek LLO
59-63 Auteurs
64 Bureau Projecten- en Rapportenregistratie
65 Hoofd Bureau Voorlichting en Public Relations
66-100 Reserve exemplaren

Contents

Abstract

Describing the effects of acidification on the level of ecosystems, the acid deposition should be available at the scale of ecosystems or at scales which allow for comparison with critical loads. Several models exist for estimating long range transport of acidifying components on a European scale (EMEP, TREND model). However, the horizontal spatial resolution of these models is too coarse to meet the needs to model the deposition on ecosystems.
In this report a description is given of the EDACS model (**E**uropean **D**eposition of **A**cidifying **C**omponents on **S**mall scale), with which the deposition of acidifying components on a small scale over Europe is calculated for 1989. The acidifying components considered in EDACS are sulphur and reduced and oxidized nitrogen compounds. Dry deposition is estimated with the inference method i.e the deposition at the surface is inferred from the concentration and the deposition velocity at the same height. The deposition velocity is calculated using a resistance model in which the transport to and absorption or uptake of a component by the surface are described. Dry deposition velocity fields over Europe are constructed from a detailed land-use map ($1/6^{o}$x$1/6^{o}$ lat/long grid, made by RIVM) and meteorological information using a detailed parameterization of the dry deposition process. These small-scale dry deposition velocity fields are combined with concentration fields from the EMEP Lagrangian long range transport model to yield dry deposition amounts on a small scale. Wet deposition is also estimated, based on measurements, to obtain a total acidifying deposition map at a European scale. These deposition fields clearly reflect the spatial detailed land-use information and the large-scale concentration pattern over Europe.
The presented deposition fields are preliminary because of several shortcomings present in the method to estimate dry deposition and data bases. An update of the deposition fields and calculations for more recent years will be available in 1995. A more thorough uncertainty analysis of the deposition maps and a validation with measurements will also be carried out. The maps of the acidifying components over Europe on a small scale are made in cooperation with the EMEP\MSC-W, Oslo, Norway.

Samenvatting

Om de effecten van verzurende stoffen op ecosystemen te beschrijven moet de depositie van deze stoffen ook op een voor ecosystemen relevante schaal (typisch enkele kilometers) zijn gegeven. De huidige modellen die het transport van verzurende stoffen over Europa beschrijven, zoals EMEP en TREND model, beschrijven deze depositie op een relatief grote schaal (tientallen kilometers). In dit rapport wordt een beschrijving gegeven van het EDACS (**E**uropean **D**eposition of **A**cidifying **C**omponents on **S**mall scale) model. Met dit model wordt de depositie van verzurende stoffen op kleine schaal over Europa berekend. Het doel van deze voorlopige kaarten is het zichtbaar maken van het detail van de verzurende depositie relevant in de effectenstudies. Met deze meer gedetailleerde depositiekaarten is een betere vergelijking mogelijk geworden met de "critical loads" over Europa.

De componenten die als verzurend beschouwd worden zijn: SO_2 and SO_4^{2-}-aerosol (SO_x), NO, NO_2 (NO_x), HNO_3 and NO_3^--aerosol and NH_3 and NH_4^+-aerosol (NH_x). De droge depositie wordt berekend met behulp van de "inference" methode. Dit betekent dat de depositie op een bepaald oppervlak bepaald wordt uit een geparametrizeerde depositiesnelheid en de concentratie, beide gegeven op een zelfde hoogte boven het oppervlak. In EDACS worden droge depositievelden over Europa berekend gebruikmakend van het RIVM landgebruikbestand op $1/6^{o}$x$1/6^{o}$ lengte-breedtegraad rooster (van de Velde *et al.* 1994) en meteorologische informatie en een gedetailleerde beschrijving van het depositieproces (i.e. depositiesnelheid). Deze parametrizaties zijn afgeleid uit experimenten (zoals uitgevoerd in het EUROTRAC/Biatex programma) en literatuurgegevens. De droge depositiesnelheidsvelden per component worden vermenigvuldigd met de concentratievelden van het EMEP Lagrangiaanse verspreidingsmodel op 150x150km resolutie. De natte depositie van verzurende stoffen is ook geschat, op basis van metingen (van Leeuwen *et al.* 1995), en toegevoegd aan de droge depositiekaarten om zo vervolgens de totale potentiële verzuringskaart over Europa te verkrijgen.

De depositievelden vertonen verscheidene ruimtelijke patronen. Deze zijn gekoppeld aan de brongebieden, meteorologische omstandigheden en het landgebruik. De onzekerheden in deze kaarten is groot aangezien er een groot aantal onzekerheden in de droge depositie-parameterizaties en de gegevensbestanden aanwezig is. Deze kaarten zijn dan ook voorlopig en zullen, in de loop van 1995 en verder, vernieuwd worden.

De verzuringskaarten op kleine schaal over Europa worden vervaardigd in samenwerking met het EMEP\MSC-W, te Oslo, Noorwegen.

1 Introduction

In Europe, sulphur and reduced and oxidized nitrogen compounds are found to acidify soils and surface waters. Furthermore, nitrogen deposition causes eutrophication. The effects of acidification and eutrophication have been described extensively in the literature (e.g. Heij and Schneider, 1991, Grennfelt and Thörnelöf, 1992). Especially the effects on ecosystems have obtained great attention due to their vulnerability. In order to protect these ecosystems critical loads have been defined above which there is an increased risk of damage to the ecosystems.

The main atmospheric pathways via which emitted acidifying components reach the earth's surface are dry and wet deposition. The acidifying components can be transported over a long range up to 1000 km or more dependent on the component properties and the dry and wet deposition processes. Several models exist for estimating long-range transport of acidifying components on a European scale (e.g. EMEP: Sandnes, 1993, TREND: van Jaarsveld and Onderdelinden, 1994). The purpose of these models is to describe the relation between source and receptor. The model results are used in quantifying country to country budgets, as a basis for the sulphur and nitrogen protocols and in assessments of the effects of acidification. The horizontal spatial scale on which these models operate is typically 50x50 km. However, describing the effects of acidification on the level of ecosystems, the acid load should be available at the scale of ecosystems or at scales which allow for comparison with critical loads (i.e. typically in the order of a 1x1 km resolution, Hettelingh *et al.*, 1991). So the above model resolutions are not appropriate to describe the acidifying load at the level of ecosystems.
A method was presented by van Pul *et al.*, 1992a, with which the deposition of acidifying components on a small scale over Europe can be mapped. Their method was discussed at the ECE-EMEP/BIATEX Workshops on deposition at Göteborg, Sweden (Lövblad *et al.*, 1993) and Aveiro, Portugal (Slanina *et al.*, 1993) and accepted as currently the best available method to describe local acid deposition fluxes.
In this report the method is described and the first, preliminary, maps of small-scale fluxes of acidifying components over Europe are presented. The calculations are made with the EDACS model (**E**uropean **D**eposition of **A**cidifying **C**omponents on **S**mall scale) in which the method is adopted. Recommendations made during the Workshops are incorporated in the model.
The emphasis in the method is on modelling local scale dry deposition fluxes. A detailed parameterization of the dry deposition process for each acidifying component is based on available experimental results (EUROTRAC/BIATEX project) and literature (Erisman *et al.* 1994a). Wet deposition is also estimated to obtain a total acidifying deposition map over Europe (van Leeuwen *et al.*, 1994). The dry deposition maps were presented at the EUROTRAC symposium at Garmisch Partenkirchen, April 1994 by Erisman *et al.*(1994b) and

van Pul *et al.*(1994a). The maps of the acidifying components over Europe on a small scale are made in cooperation with the EMEP\MSC-W, Oslo, Norway.

2 General description of EDACS

An overview of the input for and calculation scheme of EDACS is presented in Figure 1. (For a more technical description of EDACS can be found in Appendix A).
In EDACS the dry deposition is estimated with the inference method (Hicks, 1986). The deposition at the surface is inferred from the concentration and the deposition velocity at the same height. The deposition velocity is calculated using a resistance model in which the transport to and absorption or uptake by the surface of a component are described (see Section 3). The parameterizations are dependent on surface characteristics and other environmental and meteorological conditions. Dry deposition velocity fields are constructed from a detailed land-use map using these parameterizations along with the meteorological information. Here a RIVM data base is used which contains land-use data on a 1/6°x1/6° lat/long grid over Europe (van de Velde *et al.* 1994). Finally the dry deposition amounts are calculated by multiplying these dry deposition velocity fields with concentration fields.

In principle the concentration data can originate from measurements, model calculations or a combination of both. However, the spatial resolution of the operational European and national networks (ECE-EMEP, EUROTRAC) is too coarse to provide the necessary data and not every component is measured. This will lead to large uncertainties in the interpolated concentration fields. On a local scale, national or local networks may provide the concentration data. When the local maps are aggregated into one European map, problems may arise about the inconsistency between the networks and it is foreseen that still not a full coverage of Europe can be obtained. However, for parts of Europe with small horizontal concentration gradients this can be done e.g. for UK:UK Review group on acid rain, 1990; Sweden: Lövblad *et al.* 1991, The Netherlands; Erisman 1992).

In this report the concentration data of the EMEP Lagrangian long-range transport model (hence EMEP-LRT) on a 150x150 km scale were used (as described in Sandnes, 1993) to obtain a consistent concentration field over Europe. Using calculated concentration fields, the relation between emissions and deposition is maintained and assessments or scenario studies can be made at different scales.

In the inference method it is assumed that a constant flux layer is present between the reference height and the surface i.e. the atmospheric surface layer. This assumption implies that there is no significant advection in the layer and the air flow is well-adapted to the surface properties of the depositing surface and chemical reactions are not present. In that

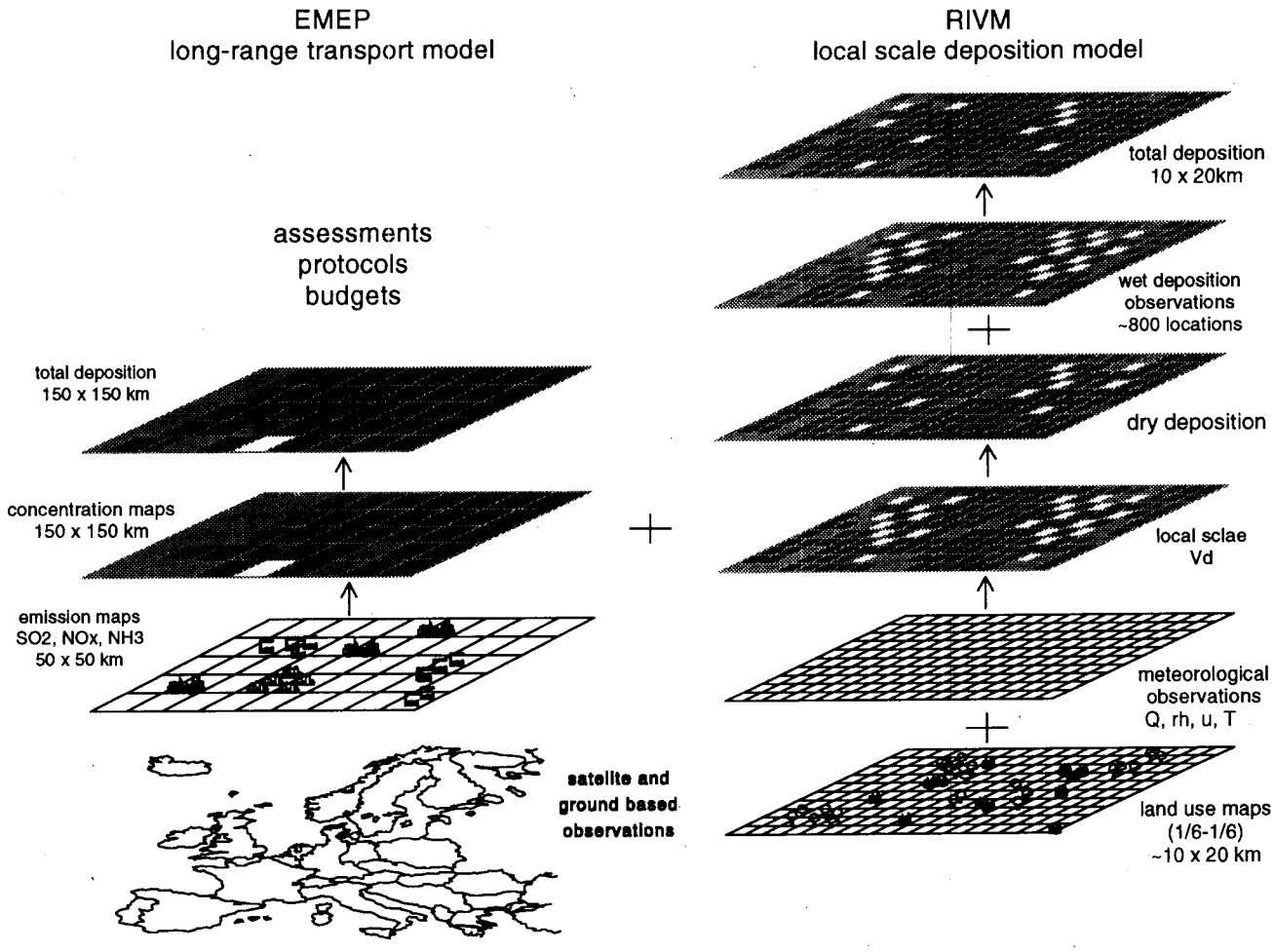

Figure 1 Overview of the input for and calculation scheme of EDACS. For explanation see text.

case the deposition flux at the reference height equals the deposition flux at the surface. The adaptation of the air flow to the surface is strongly dependent on the surface roughness and the stability of the air. The choice of the reference height is a compromise between the height where the concentration is not severely affected by local deposition and is below the surface layer height. In EDACS the concentration at 50m is taken which is the lowest LRT model level above the surface. This concentration then is assumed to be representative for a certain area, here an EMEP LRT gridcell of 150x150 km, and consequently can be used in estimating the deposition to surfaces within this area.

The wet deposition of acidifying components is based on measurements of the concentrations in precipitation and rain amounts (van Leeuwen *et al.*, 1994). A concentration map over

Europe was constructed from these data by kriging. A data set with interpolated values of long-term yearly precipitation amounts was used to calculate the wet deposition. More detail on the method can be found in Section 4.

The components considered here are SO_2 and SO_4^{2-}-aerosol (SO_x), NO, NO_2 (NO_x), HNO_3 and NO_3^--aerosol and NH_3 and NH_4^+-aerosol (NH_x). NH_x is considered to be acidifying because of the nitrification processes in the soil in which H^+ is produced (van Breemen *et al.* 1982). If all above components which are deposited produce one equivalent of acid this leads to a total potential acid load which is estimated from: potential acid = 2 SO_x + NO_y + NH_x. The actual acid load differs from the potential load because of an incomplete nitrification of NH_3 and by neutralization of the acidity by base cations. HONO, PAN and HNO_2 are not taken into account. However, the contribution of these components to the total acidifying deposition is very small (e.g. Lövblad et al., p 19).

3 Parameterization of the dry deposition velocity

The dry deposition flux of gases and particles from the atmosphere to a receptor surface is governed by the concentration in air and turbulent transport processes in the boundary layer, by the chemical and physical nature of the depositing species and by the efficiency of the surface to capture or absorb gases and particles. The flux of a trace gas is given as:

$$F = V_d(z)\ c(z) \qquad (1)$$

where c(z) is the concentration at height z and V_d is the dry deposition velocity (Chamberlain, 1966). *z* is the reference height above the surface: here taken as 50m. If the surface is covered with vegetation, a zero-plane displacement, d, is included: z=z-d. The absorbing surface is often assumed to have zero surface concentration. This holds only for depositing gases and not for gases that might also be emitted, such as NH_3 and NO. For these gases a non-zero surface concentration, a compensation point c_p, might exist, which can be higher than the ambient concentration, in which case the gas is emitted. Here the concentration at the various surfaces, c_s, is assumed to be zero for all components because of insufficient knowledge of the compensation point.

The parameterization of the dry deposition velocity is based on a description of this process via a resistance analogy or Big Leaf Model (see e.g. Thom, 1975, Hicks *et al.*, 1987, Fowler, 1978). In this resistance model the most important deposition pathways via which the component is transported and subsequently destroyed at, or taken up by the surface, are parameterized. The resistance model used here is shown in Figure 2.

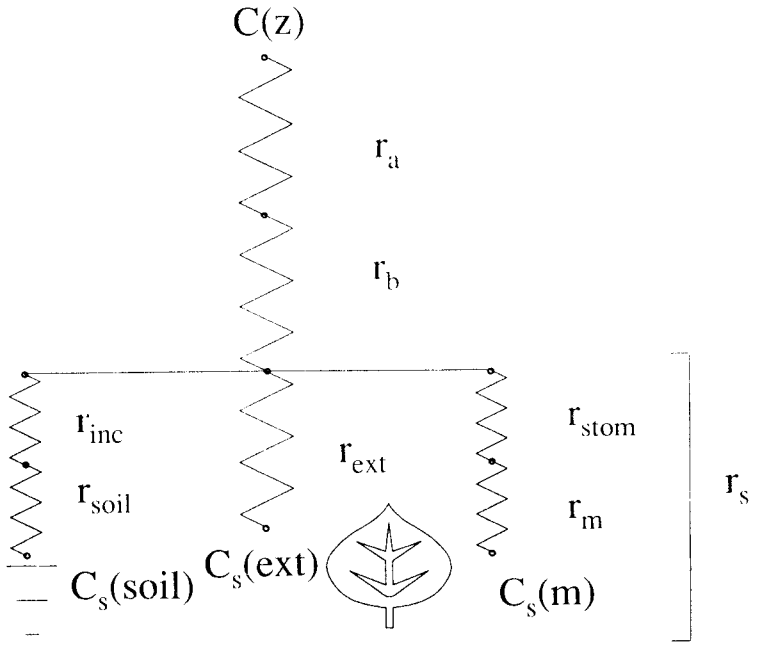

Figure 2 Resistance or Big Leaf model used in EDACS. c_s(soil), c_s(ext) and c_s(m) denote the concentration at the soil, external or mesophyl surface respectively, for explanation of the other symbols see text).

V_d is the inverse of three resistances:

$$V_d = (r_a + r_b + r_s)^{-1} \quad (2)$$

These three resistances indicate the three stages of transport: the aerodynamic resistance, r_a, represents the resistance against turbulent transport of the component close to the surface; the quasi-laminar sublayer resistance, r_b, accounts for the transport of the component through a laminar layer adjacent to the surface by molecular diffusion and the surface resistance r_s for the uptake or destruction at the surface. This surface resistance is composed of the resistances of the various destruction or uptake processes at the surface.
For a surface covered with vegetation this is:
-the stomatal resistance, r_{stom}, the resistance to the transport through the stomata of leaves and needles;
-the mesophyl resistance, r_m, the resistance of the internal plant tissues against the uptake or destruction (in a chemical way);
-the cuticle resistance, r_{cut}, or external surface resistance, r_{ext}, the resistance of the exterior plant parts against the uptake or destruction of the component;

-the r_{inc} the in-canopy aerodynamic resistance to account for the transport of air above the vegetation towards the soil and lower plant parts;
-r_{soil}, the soil resistance, the resistance against destruction or absorption at the soil surface;
These resistances which act in parallel or series are summed up to yield a (total) surface resistance, r_s:

$$r_s = \left[(r_{inc} + r_{soil})^{-1} + r_{ext}^{-1} + (r_m + r_{stom})^{-1}\right]^{-1} \quad (3)$$

For a water surface: $r_s = r_{wat}$, where r_{wat} is the resistance against the solution of gases in water.
For bare soil: $r_s = r_{soil}$ and for urban areas: $r_s = r_{urban}$. When the surface is covered with snow $r_s = r_{snow}$.

In turn, these resistances are affected by meteorology, leaf area, stomatal physiology, soil and external leaf surface pH, and presence and chemistry of water drops and films. Especially the state of the leaf and soil surface i.e. the presence of water films and snow, is an important variable in the deposition of soluble gases such as SO_2 and NH_3.

The process of dry deposition of particles of acidifying components is not very well known compared to the gaseous counterparts (Ruijgrok *et al.*,1993). As a best estimate the dry deposition of particles is described using a parameterization by Wesely *et al.*(1985) and Erisman (1992). Recent information on the deposition of particles to forests has come available (Ruijgrok *et al.* 1994) and will be used in a future version of the model.

The scheme used here to derive the surface resistances for SO_2, NO_2, NO, HNO_3, NH_3 is described in Erisman *e al.*(1994a). This scheme is based on previous publications among others Wesely (1989), Lövblad *et al.*(1993) and recent dry deposition measurements (among others in the BIATEX project of EUROTRAC). More details on the actual parameterizations used in EDACS can be found in Appendix B.

The resistances and deposition velocities are calculated with the fortran code DEPAC. Input to the deposition module is information on component type, land-use type and meteorology. Also information on the "pollution climate" of the surface can be indicated as a low or high ratio between the ammonia and sulphur concentration (denoted N/S). With this ratio the interaction of ammonia and sulphur on the deposition process of ammonia and sulphur is modelled (Erisman and Wyers, 1993)

The input to the deposition module is summed up in Table 1.

4 Wet deposition

To obtain wet deposition data, a questionnaire was sent to all organisations responsible for wet deposition monitoring in their country. The received data consisted (for all sites) of information on location (co-ordinates), type of rain sampler used (bulk or wet-only), concentrations of the elements, acidity (pH) and chemical analytical methods used. Most data were obtained for 1989. Approximately 750 measurement sites were used to compile concentration and wet deposition flux maps of non-marine sulphate, nitrate, ammonium, hydrogen, sodium, chloride, magnesium, potassium and calcium on a 50x50 km scale, using the kriging interpolation technique (van Leeuwen *et al.*, 1994).

Table 1. Input to the deposition module DEPAC

input	description
general	latitude, time (month,day,hour), pollution climate, (N/S ratio: 1=low, 2=high)
component	SO_2, NH_3, NO_2, NO, HNO_3, particles
land-use type	grass, arable, permanent crops, coniferous forest, deciduous forest, urban, desert, bare soil, water, ice
meteorology	short wave radiation (W m^{-2}) temperature at 1.5m (°C) relative humidity at 1.5m (%) windspeed at 10m (m s^{-1}) friction velocity (m s^{-1}) Obukhov length (m) surface wetness 0=dry, 1=wet, 9=snow

Because the histograms of the concentrations of different elements showed a skewed distribution, the original data were transformed to their common logarithms to stabilise

variances. Visual checks were performed on the log-transformed data (calculation of the ionic balance, and scatter plots between two elements that are strongly correlated) to investigate data quality. The sulphate concentration was corrected for the contribution of sea salt (by means of the sodium concentration), because only so-called non-marine sulphate (the fraction of the sulphate that is not neutralised by sodium) contributes to the potential acidification.

All concentrations measured with bulk samplers were corrected for the contribution of dry deposition in the funnels of bulk samplers based on correction factors available from literature (van Leeuwen et al. and references therein). Element dependent correction factors were used. For sodium and chloride different factors for near-sea and continental measurement sites were derived because sodium chloride concentrations are higher near the coast.

The corrected data were used to create the semivariograms necessary to interpolate the data over Europe using the kriging interpolation technique. The variograms clearly proved that the measurements were spatially correlated, indicating kriging to be a good interpolation technique. As concentration fields over Europe fluctuate less than precipitation fields, interpolation was performed on the concentration data instead of fluxes. An accurate interpolation of rainfall amounts was not possible with the data available in the data set, because only the data of 450 measurement sites for 1989 were available and did have a relatively poor quality. Therefore, a data set containing interpolated values of long-term yearly mean precipitation amounts, based on several thousands of measurements was used (Legates and Willmott, 1990).

After interpolation, a cross validation was carried out to investigate whether the variograms used accurately reproduce the spatial variability of the sampled observations. Interpolation errors were quantified by means of confidence intervals.

5 Data bases

In EDACS several data sets are used as is illustrated in Figure 1. In this section the origin and a brief description of the data bases are given.

5.1 Concentration data

For the concentration data the results of the EMEP Lagrangian LRT model at 50m were used. This model calculates concentrations and deposition of the acidifying components over Europe on a 150x 150 km grid (e.g. Sandnes, 1993). Daily averaged values of the concentrations of SO_2, NH_3, NO, NO_2, HNO_3, nitrate, ammonium and sulphate particles were used.

Rain water concentrations of NH_4^+, NO_3^-, SO_4^{2-} from about 750 measurement sites scattered over Europe were used to calculate wet deposition. These data were obtained via a questionaire send to all European countries (van Leeuwen *et al.*, 1994).

5.2 Precipitation data

Yearly mean precipitation amounts were taken from the EPA Global Ecosystem Data base (Legates & Willmott, 1989). Records mostly between 1920 and 1980 of 26858 independent precipitation stations were used to interpolate rain amounts with a global coverage on a 0.5 x 0.5 degree lat/long grid. These data were used along with the concentration fields to derive the wet deposition amounts.

5.3 Meteorological data

In EDACS meteorological data are used to describe among others the transport of the components to the surface and surface condition. A data base of the synoptical stations of the WMO on a global scale archived by ECMWF, Reading, UK was used. This data set contains meteorological observations at 00, 06, 12, 18 GMT. The data set contains 1306 stations over Europe of which 4 are ship-observations. The locations of the stations are depicted in Figure A2 of Appendix A. As can be inferred from the figure a relatively good coverage over Europe is present. Data used here are summerized in Table 2.

Table 2. Meteorological variables subtracted from ODS data base

variable	measurement height	units
wind speed U	10 m	m s^{-1}
total cloud cover N	-	octa
air temperature T	1.5 m	0.1 °C
dew point temperature T_d	1.5 m	0.1 °C
precipitation RR	-	0.1 mm

The data are interpolated to a 1°x 1° grid to obtain a coverage over Europe.
More details about this data set, data selection and interpolation procedure can be found in Potma, 1993.

5.4 Land-use data

This is a pan-european data base of land use in both vector format and in a 1/6°x1/6° lat/long grid made at RIVM (van de Velde *et al.*, 1994). This data base contains data from various national and international sources. The gridded version has six land-use categories (Table 3). A map of the dominant land-use types is presented in Figure 3. It can be seen that in some parts of Europe there exist some large gaps in land-use information. This will be overcome in a next release of the data base.

Unfortunately in the gridded version of the land-use type "forest" has not yet been subdivided into deciduous and coniferous. In the EDACS deposition module all forest is classified as coniferous.

The roughness length z_0 value is assigned per land-use type using a classification by Wieringa (1981) see Table 3. A typical vegetation height is also denoted which is necessary in the r_{inc} parameterization.

Table 3. Landuse types of the RIVM land-use data base and assigned roughness length and vegetation height.

land-use type	roughness length z_0 (m)	height (m)
grassland	0.03	0
arable	0.1 / 0.005 *	1
permanent crops	0.2	1
forest	2.0	20
inland water	0.0002	-
urban area	2.0	NA

* summer/winter value

A z_0 map of Europe was calculated on a 1/6°x1/6° lat/long grid constructed via area-weighted logarithmic averaging per grid (Figure 4). In this figure the high z_0 values of the forested areas in Europe can clearly be seen, e.g. in the Scandinavian countries and northern Russia.

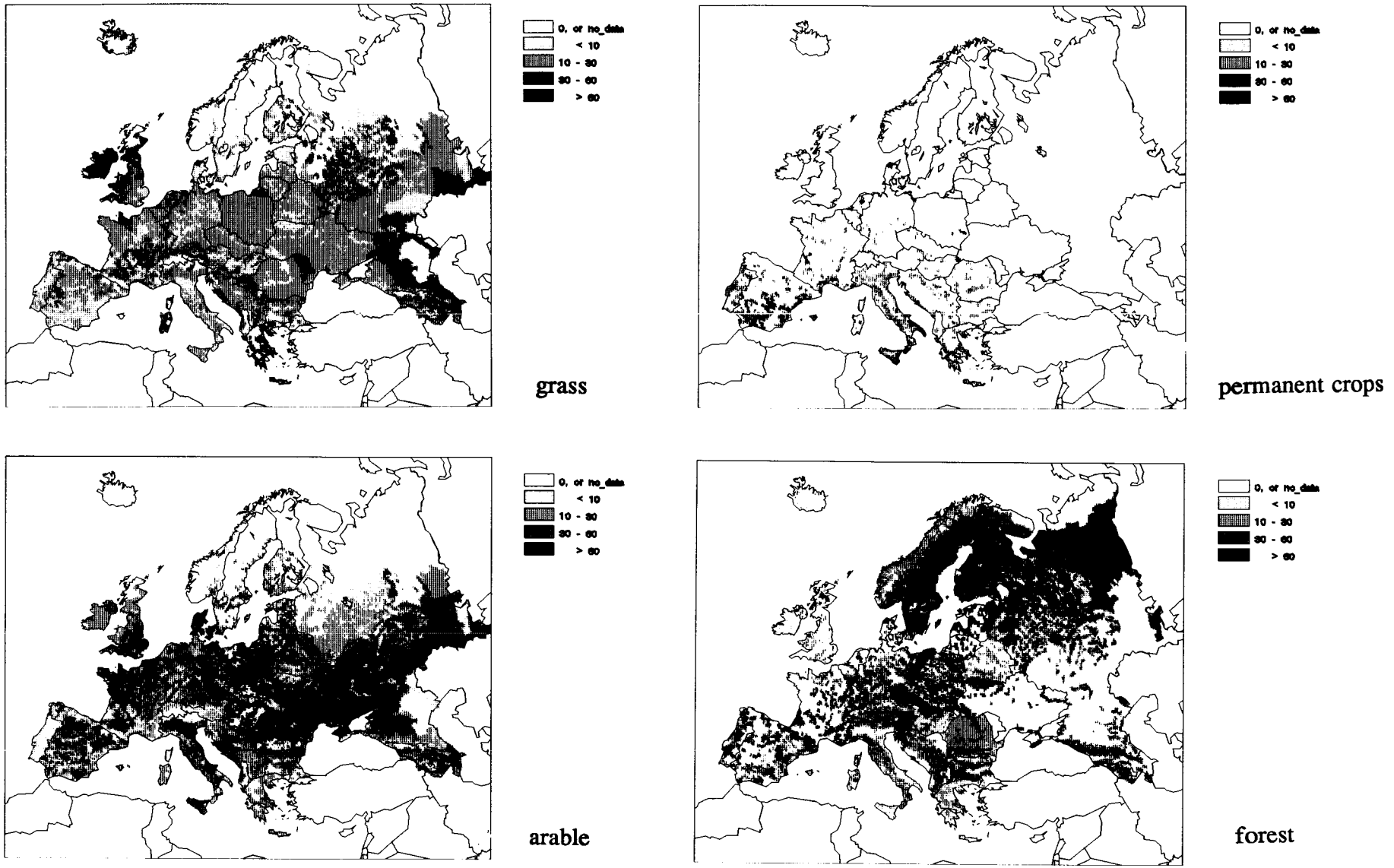

Figure 3 Dominant land-use types of the RIVM/LBG land-use data base i.e. grass, arable, permanent crops and forest given in percentages (van de Velde et al., 1994).

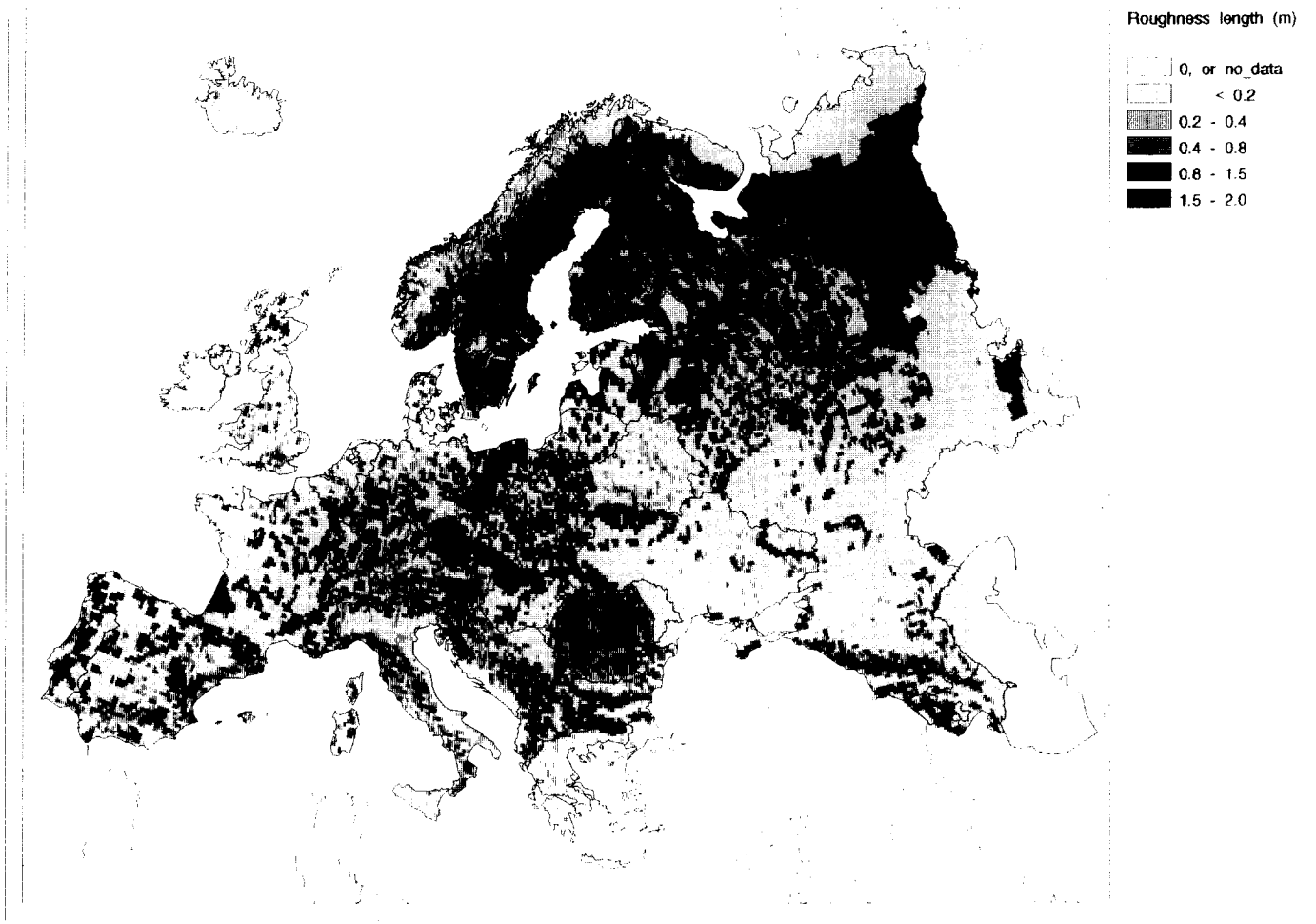

Figure 4 European rougness map (m). The z_0 value in summer for arable is used.

6 Synthesis of maps

In EDACS the calculations with and the combination of the data bases are carried out using fortran codes and Geographical Information System (GIS) procedures. Technical details are given in Appendix A.
For each land-use type in a grid cell, 6-hourly meteorological information was used to calculate the friction velocity, surface heat fluxes (sensible and latent heat) and shortwave incoming radiation. These meteorological parameters are calculated using the scheme described by Beljaars and Holtslag (1990). For this the land-use specific z_0 values were used. In DEPAC the height and LAI (Leaf Area Index) of the vegetation is needed for the calculation of the in-crop aerodynamic resistance. Since this information is not available tentative fixed values for the vegetation height per vegetation type is assumed in DEPAC, see Table 3. For the LAI a fixed value of 5 for all vegetation types was used. A simple seasonal variation of the LAI of arable and permanent crops was assumed in which the LAI linearly increases from zero in April to 5 in July and August and linearly decreases from the August-value to zero in November.

The surface wetness due to rain was taken from the synoptical data. If rain was reported the surface was assumed wet during the time period of 6 hours. Drying of the surface in the time period or information on surface wetness of the previous time period were not taken into account. As an approximation for dew occurence a simple parameterization scheme for the radiation balance of the earth's surface is used from the above routine. It is assumed that dew occurs when the latent heat flux indicated condensation. This was only used to indicate the presence of dew and was not used for estimating dew amount. In the deposition module DEPAC, no distinction is made between surface wetness caused by rain or dew.

The meteorological parameters and surface conditions are used to calculate a component specific deposition velocity at 50m for each land-use type. For each grid cell these deposition velocities are averaged, according to the land-use type percentage in the grid, to obtain one deposition velocity per grid cell. This is carried out for all components on a 6-hourly basis. Subsequently these 6-hourly deposition velocity fields were averaged to daily values. These fields are combined with the daily concentration data of EMEP/LRT to obtain dry deposition fluxes. Daily deposition fluxes were summed to annual totals.
The total wet deposition of acidifying components according to van Leeuwen *et al.*(1994) is added to the dry deposition maps to obtain an annual average total potential acidification map.

7 Preliminary results

In Figure 5 yearly average deposition velocities of SO_2, NH_3, NO_2 and particles for 1989 over Europe are depicted. From these figures it can be inferred that the deposition velocities of the components show strong variations over Europe. This is caused by variations in land use and meteorological conditions over Europe influencing the individual resistances which determine the deposition velocity. Larger deposition velocities can be seen in forested areas in Scandinavia and central Europe due to an increased turbulent exchange with the surface and so smaller resistances r_a and r_b as a result of a larger surface roughness. For particles, whose deposition velocity is parameterized solely dependent on turbulence, the pattern is also formed by a gradient in the wind speed from NW to SE. Higher dry deposition velocities of SO_2 and NH_3 are found in regions with more periods with surface wetness and longer wetness duration i.e. north western Europe. Surface wetness duration leads to smaller surface resistances of these soluble gases.

In Figure 6 the dry deposition of sulphur, oxidized and reduced nitrogen and total potential acid over Europe estimated with EDACS are shown. The dry deposition values for most components vary greatly over Europe. This is partly explained by the above variation in the deposition velocity but also by the concentration pattern of the components over Europe which are associated with the distribution of emissions. Large emission areas can be detected in the maps e.g. for SO_2 and NO_2 this is the so-called black triangle (Eastern Germany - Poland - Czech Republic), for ammonia e.g. north western Europe (The Netherlands, Denmark).

The total wet deposition of acidifying components according to van Leeuwen *et al.* (1994) is presented in Figure 7. The gaps in the map are caused by insufficient data available to carry out the kriging interpolation. The wet deposition pattern resemble European emission and weather patterns. Again the large emission areas can be recognised e.g. sulphate and nitrate emissions in the black triangle. Some high values in the wet deposition maps are induced by high rain amounts caused by the orography e.g. former Yugoslavia, Switzerland.

The total potential acidification map which is the sum of the dry deposition (Figure 6) and wet deposition (Figure 7) is presented in Figure 8. This figure reflects all the above variations. The relative contribution of dry and wet deposition can be observed. For instance in the Scandinavian countries the surface inhomogeneities are not represented due to the large contribution of the wet deposition which has a smooth distribution over this area.

The standard deviation of the total deposition of EDACS cells in an EMEP-grid cell (about 100 EDACS cells in one EMEP-grid) is given as absolute values and values relative to the average per EMEP-grid (Figure 9). It can be seen that the largest absolute values of the

standard deviation can be found in the above described emission areas. Whereas the relative standard deviation is largest in areas with a small deposition and so variations in land use, meteorology etcetera are reflected.

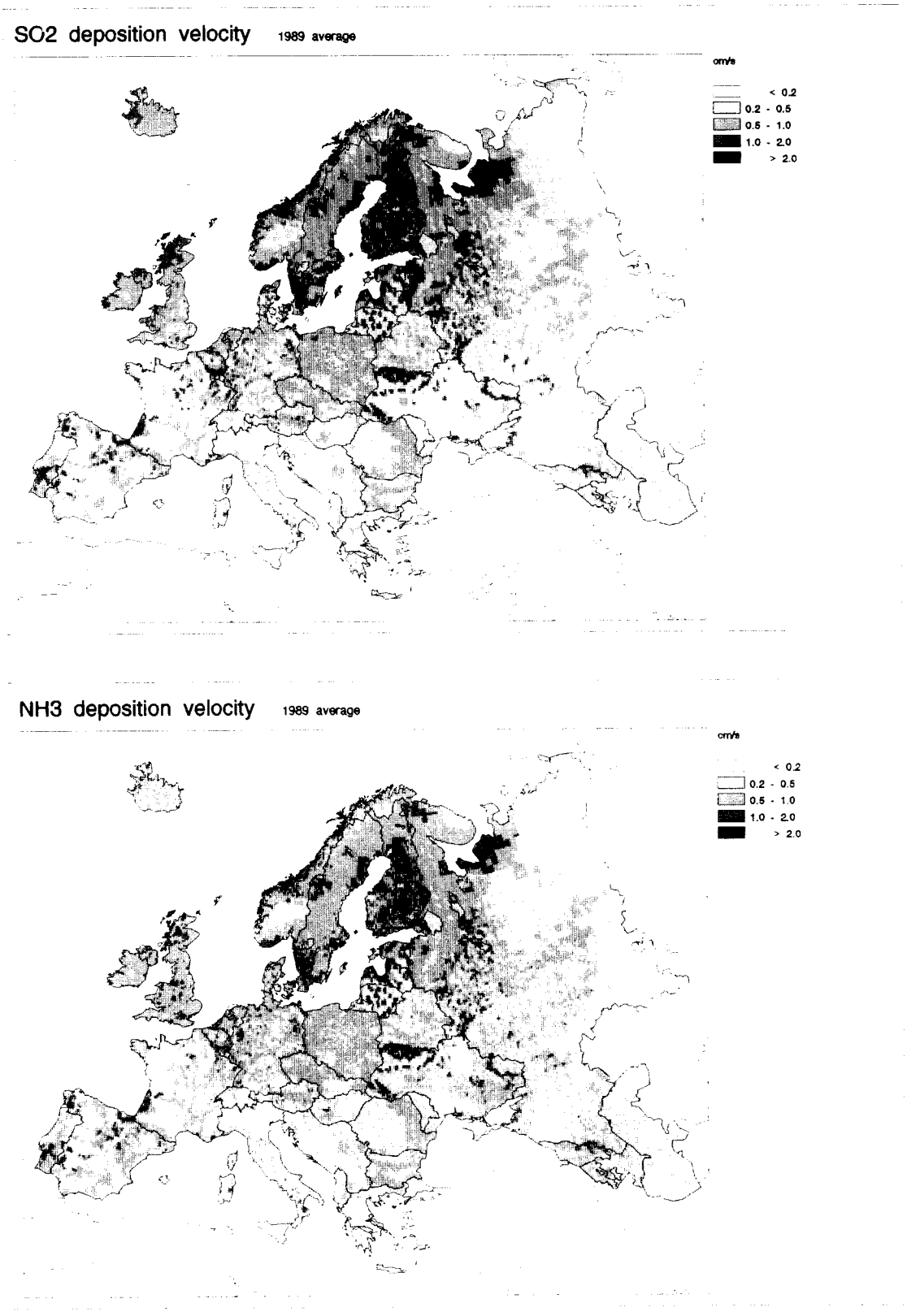

Figure 5 Yearly average deposition velocity of SO_2 (above) and NH_3 (below) over Europe for 1989 ($cm\ s^{-1}$).

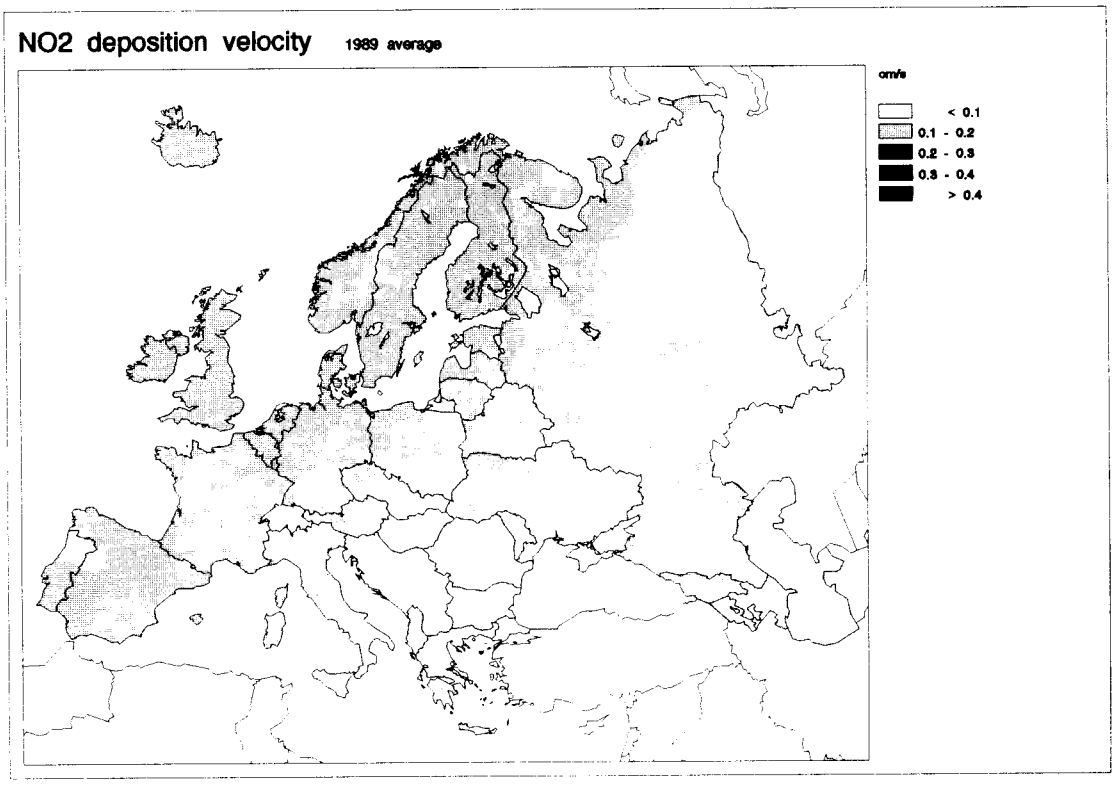

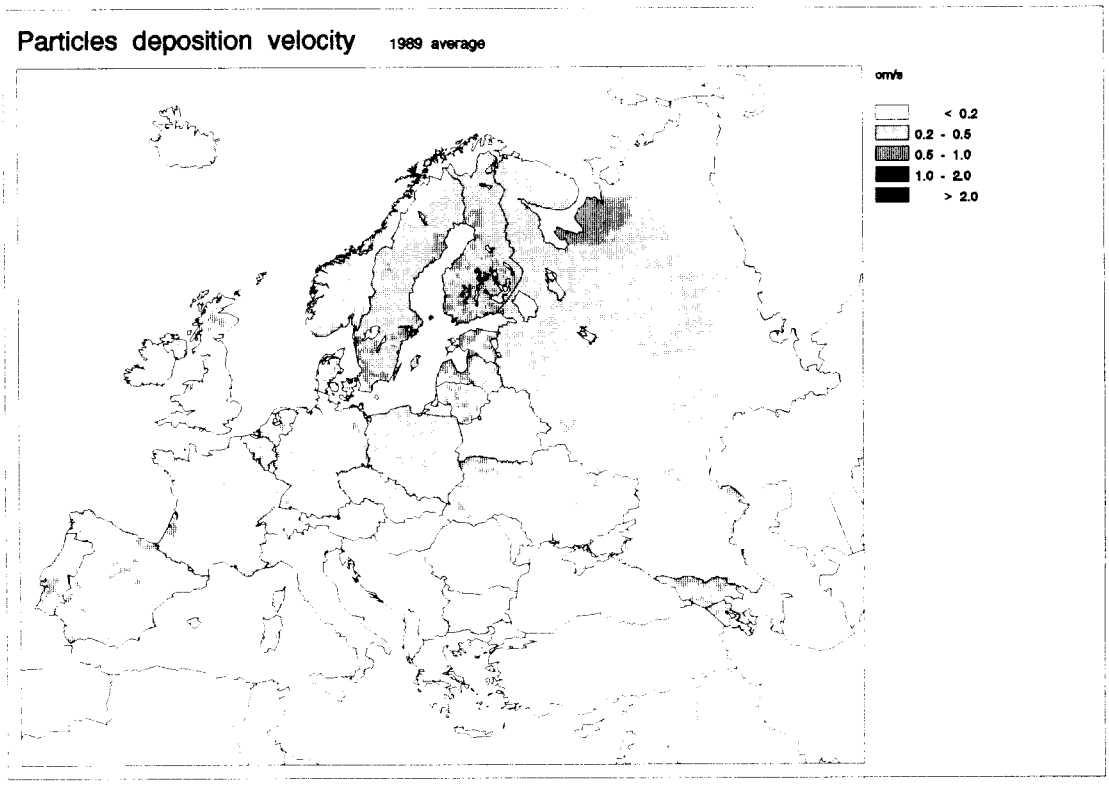

Figure 5 continued. Yearly average deposition velocity of NO_2 (above) and particles (below) over Europe for 1989 (cm s^{-1}).

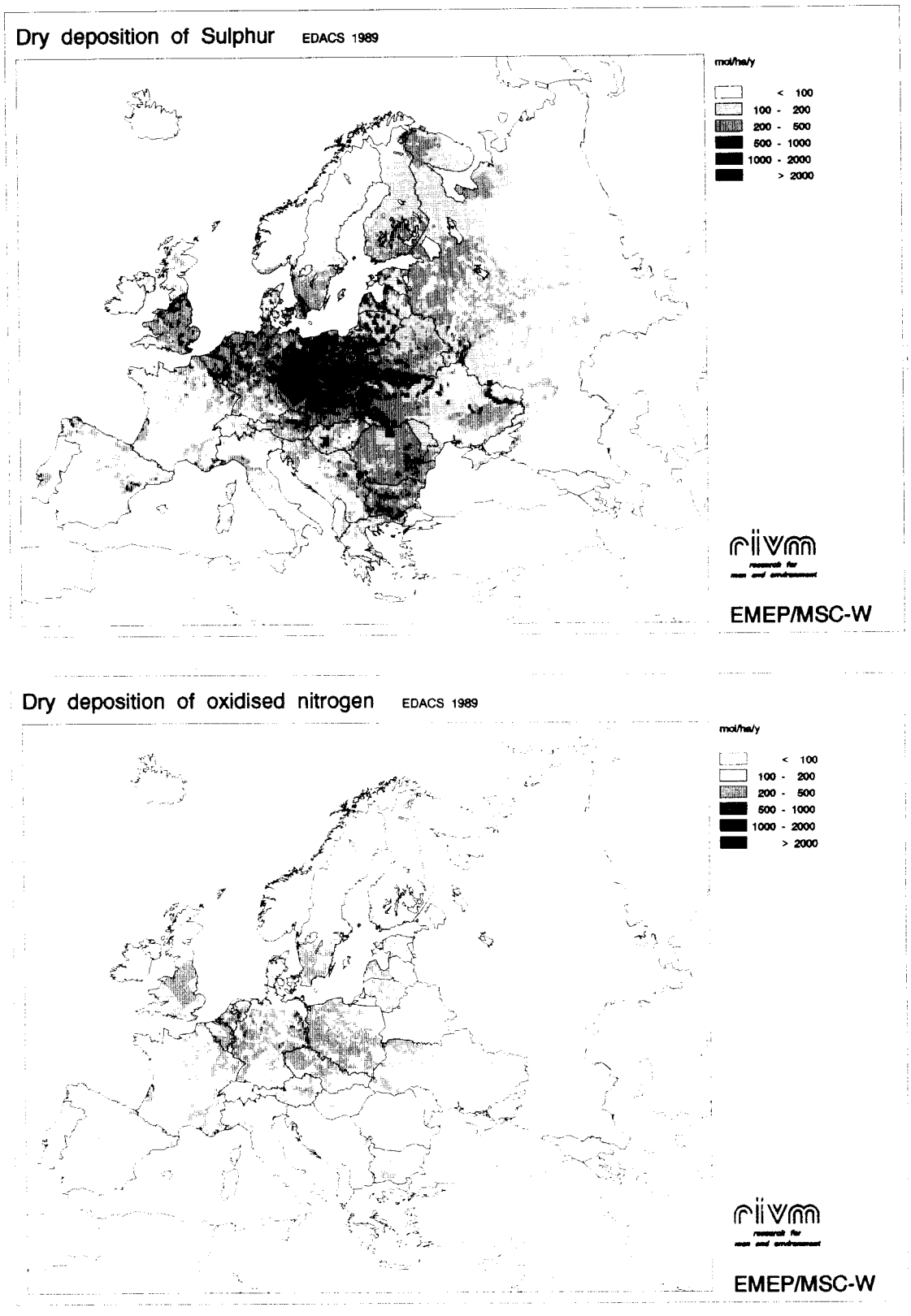

Figure 6 Dry deposition of sulphur (above) and oxidized nitrogen (below) over Europe for 1989 (mol ha^{-1} $year^{-1}$).

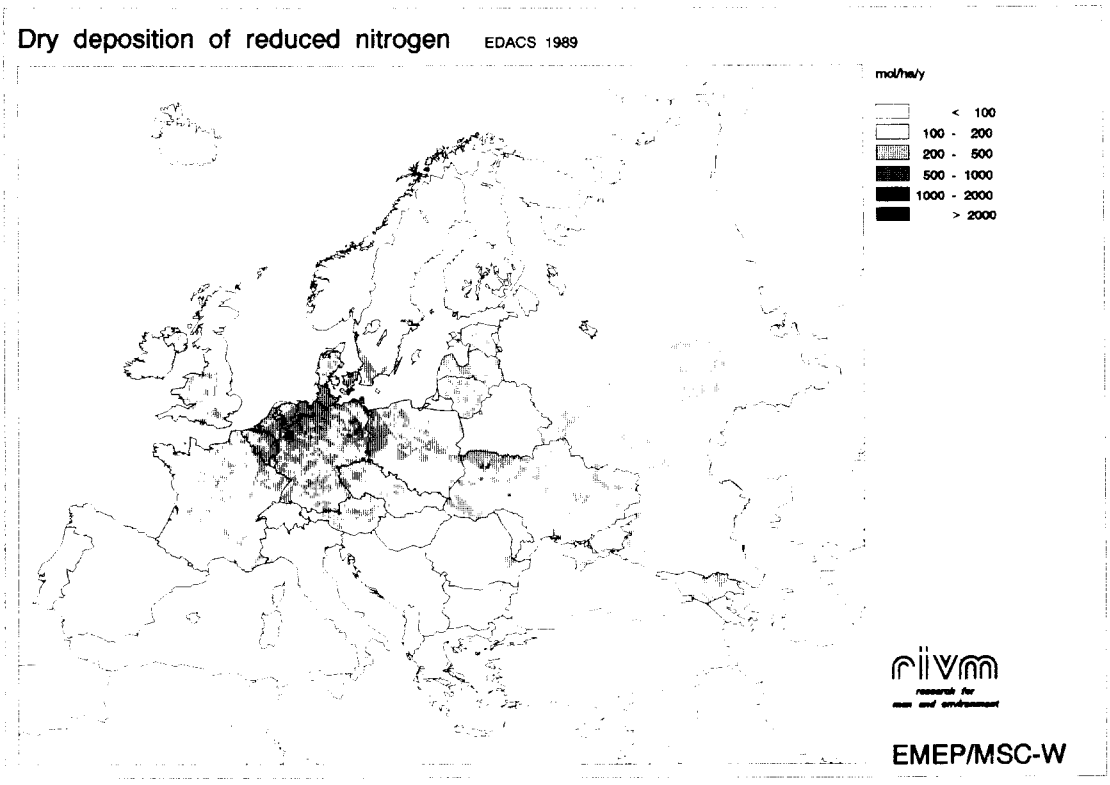

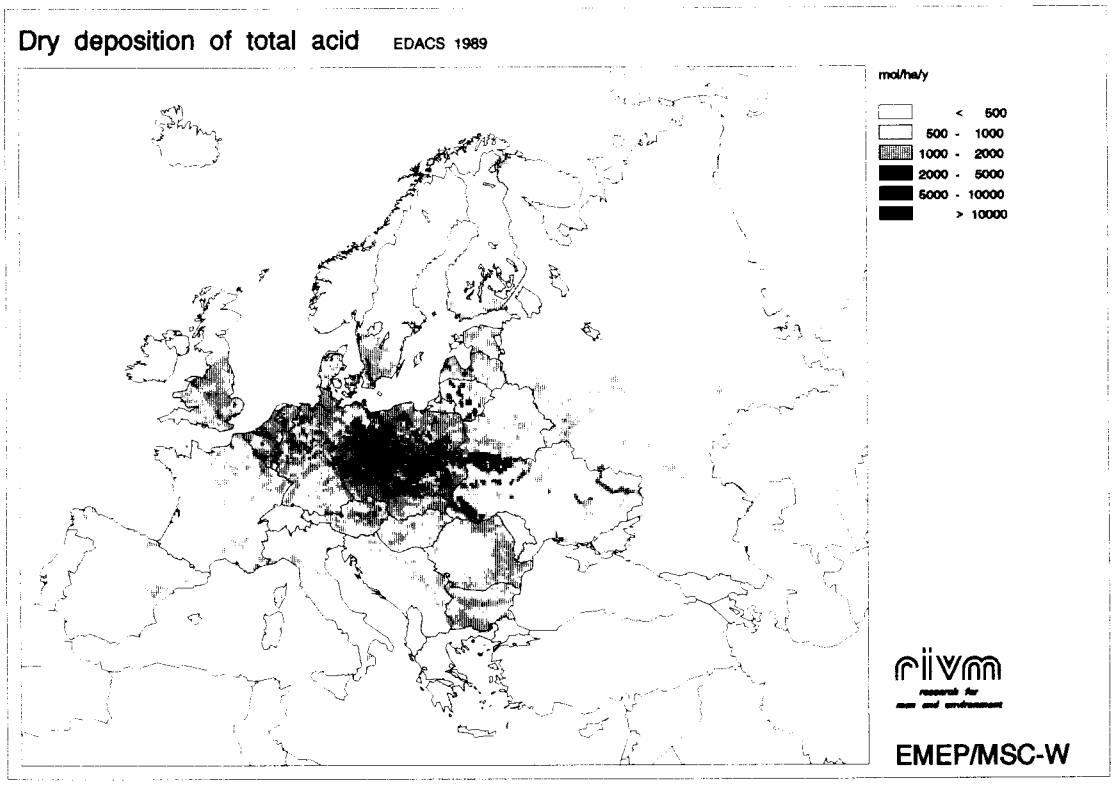

Figure 6 continued. Dry deposition of reduced nitrogen (above) and total potential acid (below) over Europe for 1989 (mol ha^{-1} $year^{-1}$).

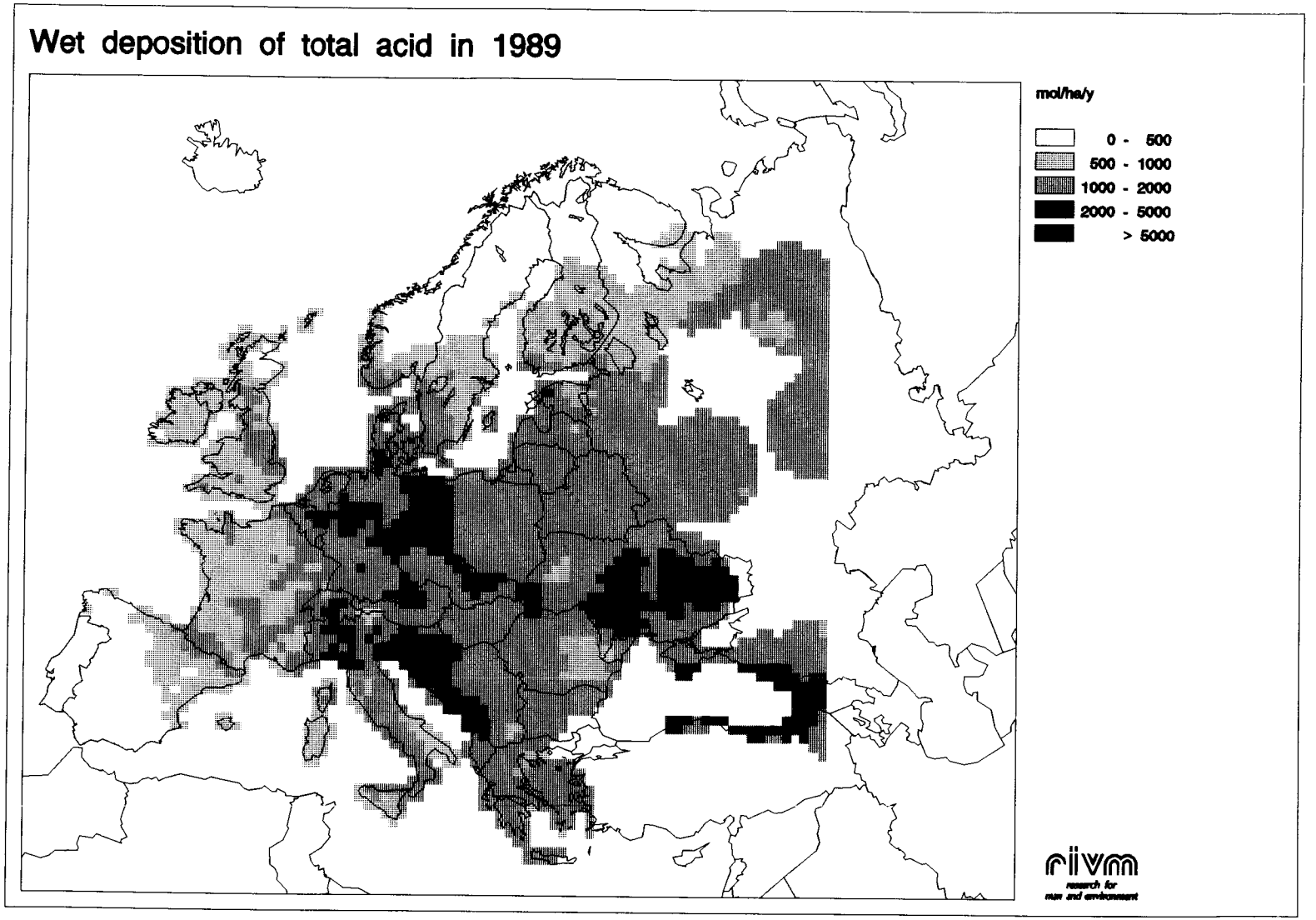

Figure 7 Total wet deposition estimated from rain concentration measurements of 1989 and long term rain fall amounts (van Leeuwen et al., 1994, Section 6 in mol ha^{-1} year^{-1}).

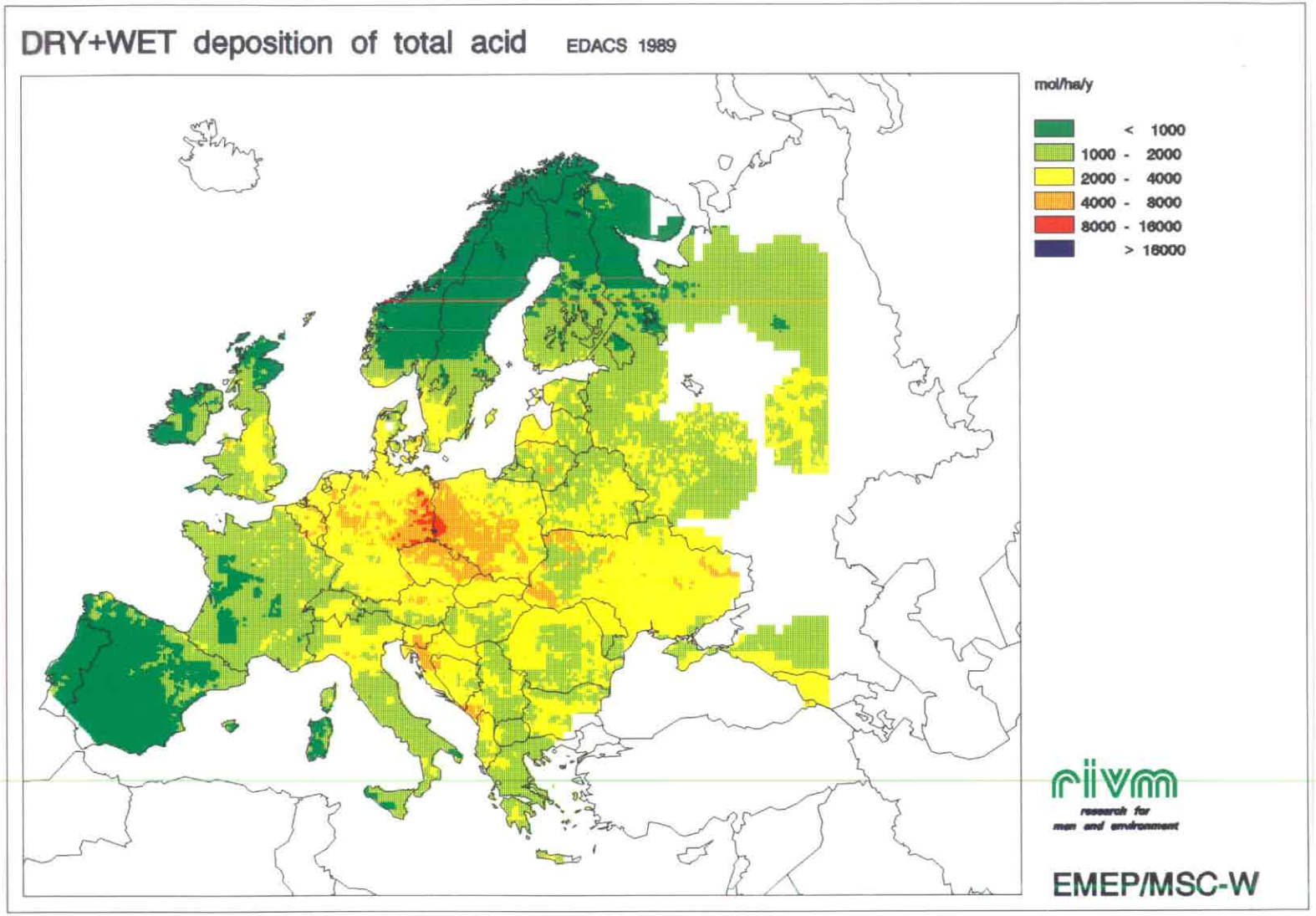

Figure 8 Potential acidification map over Europe on 1/6°x1/6° lat/long grid for 1989 (mol ha^{-1} $year^{-1}$).

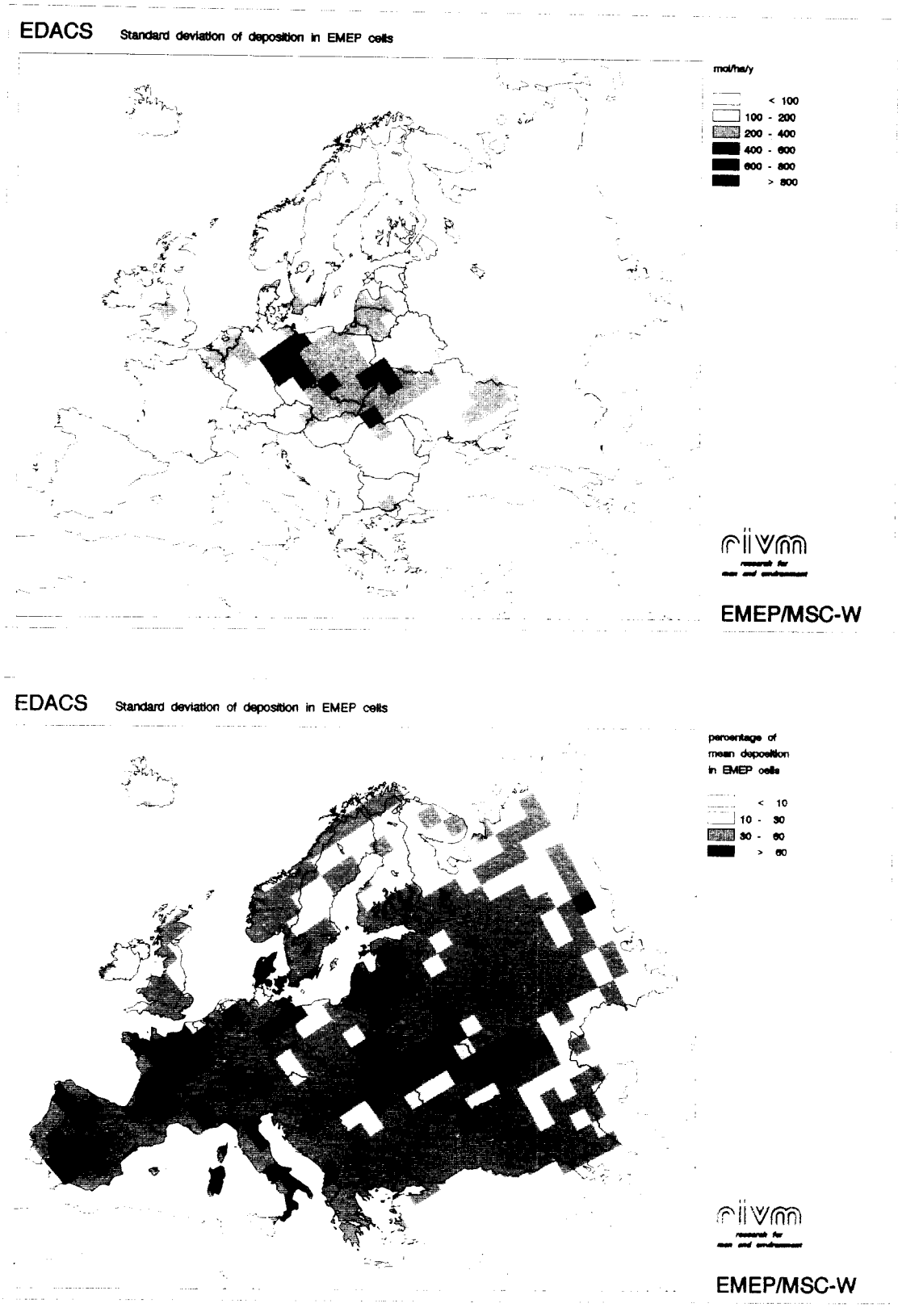

Figure 9 Standard deviation of the total deposition of EDACS grid cells per EMEP grid in absolute values in mol ha^{-1} year^{-1} (above) and values relative to the total deposition per EMEP-grid cell in % (below).

8 Uncertainties

The maps shown in Section 7 have a limited accuracy and are therefore preliminary. The aim of these maps is to show the variations of the deposition of acidifying components on a small scale. Several uncertainties and shortcomings are present which need some discussion. We will adress these items here and will suggest a quantification of the uncertainties. Also some recommendations for improvements of these maps are given.

One of the main uncertainties in the maps is in the simple resistance model and especially the surface resistance parameterization for estimating the dry deposition of different gases and particles. The resistance model is a simple approach for a highly variable process. It assumes a constant flux layer, i.e. there are no surface inhomogeneities, edge effects or chemical reactions. How much these simplifications contribute to the total uncertainty in the annual average deposition fluxes has not been investigated. The uncertainty in the surface resistance parameterization is the largest uncertainty in this simplified scheme. Therefore more, and more accurate, parameterizations are needed for various vegetations and surfaces. Moreover there is a lack of measurements on which these parameterizations can be based especially for southern and eastern European climates and surfaces. This is needed to obtain parameterizations for use in LRT models which are valid for the whole of Europe. Part of the uncertainty in the surface resistance parameterization is due to the mismatch between the available parameterizations for a limited number of landcover types and the landuse classifications used in the RIVM land-use data base.
Surface wetness is found to be one of the major factors influencing the deposition process. In the present version of EDACS only rain and an indication of dew is used. In the next version the dew amount will be modelled in more detail using appropriate surface properties. The evaporation of rain and dew will also be parameterized. This means that an administration of the available energy and moisture flux during the day has to be made. An indicator on the presence and condition of a snow layer will also be taken into account.
The overall uncertainty in the surface resistance due to the above factors is different for each component and surface type. This uncertainty, on a annual basis, is a few tens percent points but can easily exceed 100%.

In the current version of EDACS, the EMEP-LRT concentration maps on a 150x150 grid are used. The uncertainty in the concentrations are estimated at 40-70% by a statistical analysis with the EMEP measurements (Krüger, 1993). These concentrations represent the background situation in Europe. It is assumed that the concentration distribution within a grid is homogeneous. This is not the case in a grid which contains industrialised areas or many scattered sources such as of NH_3 and NO_x. For such conditions, subgrid concentration variations are present and will lead to underestimates of the deposition in that grid. To obtain an indication of the errors, a small-scale, short-range model can be useful here to resolve sub-

grid concentration gradients for dense source areas. The uncertainty in the deposition in an EDACS grid cell due to these gradients is estimated at 25% (Berg and Schaug, 1994).

The deposition in EDACS is based on the EMEP-LRT concentrations which in turn are dependent on EMEP deposition estimates. The deposition in the EMEP-LRT model and in EDACS are calculated in different ways. By using other dry deposition velocities in EDACS a mass inconsistency, between the EMEP calculated deposition and the small scale maps by EDACS, is introduced. However, if the differences in the used deposition descriptions between the two models are not very large and non-systematic over a larger region, this will not lead to large mass inconsistencies. In Figure 10 a comparison between the sulphur dry deposition per country estimated by EMEP and EDACS is shown. It can be seen that on average there is a good agreement indicating that for the model area the mass consistency is not violated to a large extent. However, for some countries the deviations can be as large as 50%. To avoid this mass inconsistency it is planned to implement the deposition module in the EMEP-LRT model. In this way the calculated concentration fields are consistent with the EDACS deposition description.

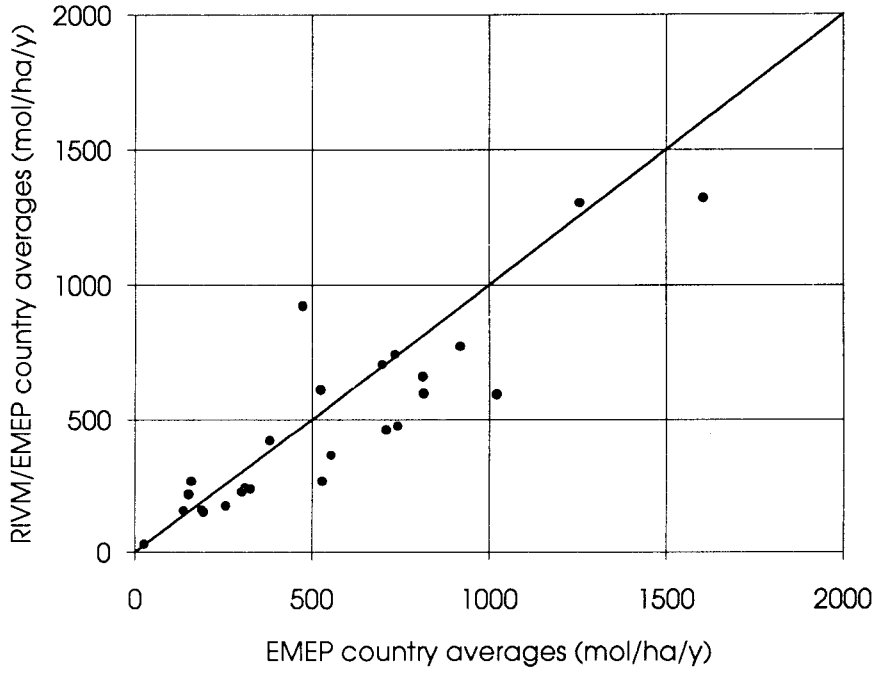

Figure 10 Comparison between the country averaged dry deposition of sulphur calculated with EMEP and EDACS (deposition in mol ha^{-1} year^{-1}).

In inferential modelling the concept is used that the surfaces, at which the deposition is calculated, should have a certain horizontal length. As an approximation this is about 100 times the reference height (Pasquill, 1972). The typical horizontal length scale of the surface, using 50m as the reference height, is 5 km. This means that only surfaces with larger length scales are modelled correctly. Variations in land cover on this scale are regularly present. At each surface transition the deposition is altered. Especially forest edges give rise to large enhancements of the deposition. This enhanced deposition can be dealt with in a very simplified way using correcting factors defined by e.g. van Pul *et al.* 1992b, Draaijers *et al.*, 1994. Since in this land-use data base only percentages of the land-use type per grid are given and not the geographical position, only a statistical approach of the uncertainty can be carried out. For instance, the enhanced deposition at forest edges as a whole for all forest stands in the Netherlands, is estimated at 10-30% (van Pul *et al.*, 1992b, Draaijers *et al.* 1994).

The accuracy of the presented results depends on the availability and quality of the input data such as the land-use map and the meteorological observations. In the gridded version of the RIVM land-use data base, forest is not subdivided into deciduous and coniferous. All forest is classified as coniferous forest. This will probably lead to overestimates of the deposition velocity to deciduous forests for all components during winter. However, the stomatal resistance in winter will be large due to low temperatures. So this overestimate will be somewhat leveled out. A version in which the forest data are subdivided in the above categories will be available in 1995. In this new version the quality of the land-use data for some areas in Eastern Europe will also be improved.

The dry deposition is calculated on a daily basis. However, due to the daily averaging of the concentration and the deposition velocity, a loss in temporal correlation is introduced between the concentration and the deposition velocity. This error is component specific and is estimated to be smaller than 20% (van Pul *et al.*,1993). In the future the deposition will be calculated on a 6-hourly basis and the above error avoided.

The uncertainty in the wet deposition estimates is relatively small compared to the uncertainty in the dry deposition estimates. A comparison between the derived wet deposition maps and EMEP long-range transport model results was carried out by means of calculation of differences and ratios between the grids derived by the two methods (van Leeuwen *et al.*, 1994). In most parts of Europe deviations were found smaller than 200 mol/ha/year in absolute terms for individual components and smaller than 50% in relative terms. The uncertainty in the wet deposition is most important in areas where wet deposition is equal to or higher than dry deposition. In such areas, however, wet deposition usually shows a smooth pattern. This is not true for mountainous regions where additional deposition pathways such as fog and cloud deposition are present. Corrections can be applied to the wet deposition if local data on fog and cloud composition, occurrence and liquid water content are available

(Fowler, 1991).

The overall uncertainty in the depostion maps consists of the above-mentioned uncertainties. However, the uncertainty in the surface resistance and the occurence of sub-grid concentration gradients will act as the largest uncertainty sources. Given these uncertainty estimates, the uncertainty in the deposition of a component of a 1/6°x1/6° lat/long gridcell is typically 100-200%. However, the uncertainty in the total potential acidification map is smaller because the total acidification consists of components such as wet deposition which have a smaller uncertainty . Erisman (1992) estimated the uncertainty in the yearly average total potential acid deposition which was also estimated with an inference method, at 45-80% for 5x5km grids in the Netherlands. This uncertainty is lower because the deposition estimates were based on more detailed spatial and temporal data.

9 Conclusions

In this report a description is given of the EDACS model, with which the deposition of acidifying components on a small scale over Europe is calculated. Dry deposition velocity fields are constructed from a detailed land-use map (1/6°x1/6° lat/long, made by RIVM) and meteorological information using a detailed parameterization of the dry deposition process. These small-scale dry deposition velocity fields are combined with air-concentration fields (taken from the EMEP Long range transport model) to yield dry deposition amounts on a small scale. Wet deposition is also estimated to obtain a total acidifying deposition map over Europe (van Leeuwen *et al.*, 1994). These deposition fields clearly reflect the spatially detailed land-use information and the large-scale concentration pattern over Europe. With these fields a better match is obtained between the critical and actual loads when ecosystems are concerned.

The presented deposition fields are preliminary because of several shortcomings present in the method and data bases. An update of the deposition fields and calculations for more recent years will be available in 1995. A more thorough uncertainty analysis of the deposition maps, a validation with (throughfall and micro-meteorological) measurements and corrections on the wet deposition caused by cloud and fog deposition will also be carried out.

Acknowledgements

A.Eliassen, E.Berge and H.Styve of EMEP MSC-W are thanked for their cooperation in providing the model concentration data. The ECMWF and KNMI are acknowledged for the WMO synops data. F.de Leeuw is acknowledged for his comments on the draft and J.Burn for editing the manuscript.

10 References

Baldocchi D.D., B.B.Hicks, and P.Camara, 1987. A canopy stomatal resistance model for gaseous deposition to vegetated surfaces. Atmospheric Environment **21**,91-101.

Beljaars A.C.M. and A.A.M.Holtslag, 1990. Description of a software library for the calculation of surface fluxes. Environ. Software **5**,60-68.

Berg,T. and J.Schaug, 1994. Proceedings of the EMEP Workshop on the Accuracy of measurements, Passua, Germany, 22-26 November 1993. EMEP/CCC report 2/94.

Breemen,N.van, P.A.Burrough, E.J.Velthorst,H.F.van Dobben, T.de Wit,T.B.Ridder and H.F.R.Reinders, 1982. Soil acidification from atmospheric ammonium sulphate in forest canopy throughfall. Nature,299,548-550.

Chamberlain A.C., 1966. Transport of gases from grass and grass-like surfaces Proc. R. Soc. Lond. A290, 236-265.

Draaijers,G.P.J.,R.van Ek, and W.Bleuten, 1994. Atmospheric deposition in complex forest landscapes. Boundary-Layer Meteorology 69, 343-366.

Erisman J.W., 1992. Atmospheric deposition of acidifying compounds in the Netherlands. PhD-thesis. University of Utrecht, the Netherlands.

Erisman J.W. and G.P. Wyers, 1993. Continuous measurements of surface exchange of SO_2 and NH_3; implications for their possible interaction in the deposition process. Atmospheric Environment 27A, 1937-1949.

Erisman, J.W.,W.A.J. van Pul and G.P.Wyers, 1994a. Parameterization of surface resistance for the quantification of atmospheric deposition of acidifying pollutants and ozone. Atmospheric Environment Vol. 28, No.16: 2595-2607.

Erisman, J.W.,C.J.M.Potma, G.P.J.Draaijers, E. van Leeuwen and W.A.J. van Pul., 1994b. A generalised description of the deposition of acidifying pollutants on small scale in Europe. In Proceedings of EUROTRAC symposium'94, P.Borrell (Ed.), SPB Academic Publishing, The Hague, the Netherlands.

Erisman J.W., 1994c. Evaluation of a surface resistance parameterization for SO_2, Atmospheric Environment Vol.28, No.16: 2583-2594.

Erisman J.W. and Baldocchi D.D., 1994d. Modelling dry deposition of SO_2. Tellus 46B, 159-171.

Fowler D., 1978. Dry deposition of SO_2 on agricultural crops. Atmospheric Environment 12,369-373.

Fowler D., J.H.Duyzer, D.D.Baldocchi, 1991. Inputs of trace gases, particles and cloud droplets to terrestrial surfaces. Proc. R. Soc. Edinburgh 97B,35-59.

Grennfelt,P. and E.Thörnelöf, 1992. Critical loads for Nitrogen. Report from a workshop at Lökeberg, Sweden, April 6-10, 1992. Report No. Nord 41, Nordic Council of Ministers, Copenhagen.

Heij, G.J. and T.Schneider (Ed.), 1991. Acidification research in the Netherlands. Studies in Environmental Science 46. Elsevier,Amsterdam.

Hettelingh,J.P.,R.J.Downing and P.A.M.de Smet, 1991. Mapping critical loads for Europe. CEC technical report no.1 RIVM report 259101001.

Hicks, B.B.,1986. Measuring dry deposition: a re-assessment of the state of the art. Water,Air and Soil Pollution 30: 75-90.

Hicks B.B., D.D.Baldocchi, T.P.Meyers, R.P.Hosker Jr. and D.R.Matt, 1987. A preliminary multiple resistance routine for deriving dry deposition velocities from measured quantities. Water Air Soil Pollut. 36, 311-330.

Hicks B.B., R.R.Draxler, D.L.Albritton, F.C.Fehsenfeld, J.M.Hales, T.P.Meyers, R.L.Vong, M.Dodge, S.E.Schwartz, R.L.Tanner, C.I.Davidson, S.E.Lindberg and M.L.Wesely, 1989. Atmospheric processes research and process model development. State of Science/Technology, Report no. 2. National Acid Precipitation Assessment Program.

Jaarsveld, J.A. van and D.Onderdelinden, 1994. An analytical long term deposition model for multi-scale applications. RIVM report in preparation.

Krüger,O., 1993. The application of the EMEP-model to estimate budgets for airborne acidifying components in Europe. In: Proceedings CEC/BIATEX Workshop 4-7 May 1993 Aveiro, Portugal. Ed. J.Slanina. pp 31-38.

Lövblad, G.,J.W.Erisman and D.Fowler, 1993. Models and methods for the quantification of atmospheric input to ecosystems. Proceedings Nordic Council/EMEP/BIATEX workshop in Götenborg 3-6 November 1992.

Leeuwen, E.P. van, J.W.Erisman, G.P.J.Draaijers, C.J.M.Potma and W.A.J.van Pul, 1994. European wet deposition maps based on measurements. Report no. 722108008. RIVM, Bilthoven, the Netherlands. (in preperation)

Legates, D.R. and C.J. Willmott, 1990. Mean seasonal and spatial variability in gauge-corrected, global precipitation, International Journal of Climatology, Vol.10: 111-123.

Pasquill,F., 1972. Some aspects of boundary-layer description. Quarterly Journal of the Royal Meteorological Society 98:469-494.

Potma, C.J., 1993. Description of the ECMWF/WMO Global Observational Data Set and associated data extraction and interpolation procedures. RIVM report 722401001.

Pul W.A.J. van, J.W.Erisman, J.A. van Jaarsveld and F.A.A.M. de Leeuw, 1992a. High resolution assessment of acid deposition fluxes. In Acidification research: evaluation and policy application. (edited by T. Schneider), Studies in Environmental Science. Elsevier, Amsterdam.

Pul W.A.J. van, R.M.van Aalst and J.W.Erisman, 1992b. Deposition of air pollution at a forest edge: a simple approach. In: J.Slanina,ed., EUROTRACK/BIATEX annual report,Garmisch-Partenkirchen, FRG 248-254.

Pul W.A.J. van, J.W.Erisman, J.A. van Jaarsveld and F.A.A.M. de Leeuw, 1993. Methodology for mapping acidifying components over Europe. In: Proceedings CEC/BIATEX Workshop 4-7 May 1993 Aveiro, Portugal. Ed. J.Slanina. pp 95-115.

Pul W.A.J. van and A.F.G. Jacobs, 1994. The conductance of a maize crop and the underlying soil to ozone under various environmental conditions. Boundary-Layer Meteorology

69: 83-99.

Pul W.A.J. van, C.J.M.Potma, G.P.J.Draaijers, E. van Leeuwen and J.W.Erisman, 1994. Small scale deposition fluxes of acidifying components over Europe. In Proceedings of EUROTRAC symposium'94, P.Borrell (Ed.), SPB Academic Publishing, The Hague, the Netherlands.

Ruijgrok W. and C.I.Davidson C.I., 1993. Particle deposition. In Proceedings Nordic Council/EMEP/BIATEX workshop, Götenborg, Sweden, 3-6 November 1992. Ed. Lövblad, G., J.W.Erisman and D.Fowler.

Ruijgrok W., H.Tieben and P.Eisinga, 1994. Dry deposition of acidifying and alkaline particles to Douglas fir: a comparison of measurements and model results. Report 20159-KES/MLU, KEMA, Arnhem, the Netherlands.

Sandnes H., 1993. Calculated budgets for airborne acidifying components in Europe, 1985, 1987, 1988, 1989, 1990, 1991 an 1992. EMEP report 1/93. MSC-West, Oslo, Norway.

Slanina, J., G.Angeletti and S.Beilke, 1993. General Assessment of biogenic emissions and deposition of nitrogen compounds, sulphur compounds and oxidants in Europe. Proceedings CEC/BIATEX Workshop 4-7 May 1993 Aveiro, Portugal.

Thom A.S., 1975. Momentum, mass and heat exchange of plant communities. In: Vegetation and Atmosphere, pp. 58-109 (Ed. Monteith J.L.), Academic Press, London.

UK Review Group on Acid Rain, 1990. Acid deposition in the United Kingdom. Warren Spring Laboratory, Stevenage, UK.

Velde van de, R.J., W.Faber, V.Katwijk, H.J.Scholten, T.J.M.Thewessen, M.Verspuy and M.Zevenbergen, 1994. The preparation of a European Land-use Data base, report

report 712401001, RIVM, Bilthoven, the Netherlands.

Voldner E.C., L.A.Barrie and A.Sirois, 1986. A literature review of dry deposition of oxides of sulfur and nitrogen with emphasis on long-range transport modelling in North America. Atmospheric Environment 20,2101- 2123.

Walcek, C.J., R.A.Brost, J.S. Chang and M.Wesely, 1986. SO_2, sulfate and HNO_3 deposition velocities computed using regional landuse and meteorological data. Atmospheric Environment 20, 949-964.

Wesely M.L., D.R.Cook and R.L.Hart, 1985. Measurements and parameterization of particulate sulphur dry deposition over grass. J. geophys. Res. 90,2131-2143.

Wesely M.L., 1989. Parametrization of surface resistances to gaseous dry deposition in regional-scale numerical models. Atmospheric Environment 23,1293-1304.

Wieringa J., 1981. Estimation of mesoscale and local-scale roughness for atmospheric transport modelling. Air pollution modelling and its application (edited by Wispelaere C. de),pp. 279-295. Plenum Publishing Corp., New York.

Appendix A Technical description of EDACS

EDACS is a combination of data bases, fortran programs and Geographical Information System (GIS) procedures. In this appendix, the overall structure of EDACS will be described. A general outline of the EDACS system is shown in Figure A1.

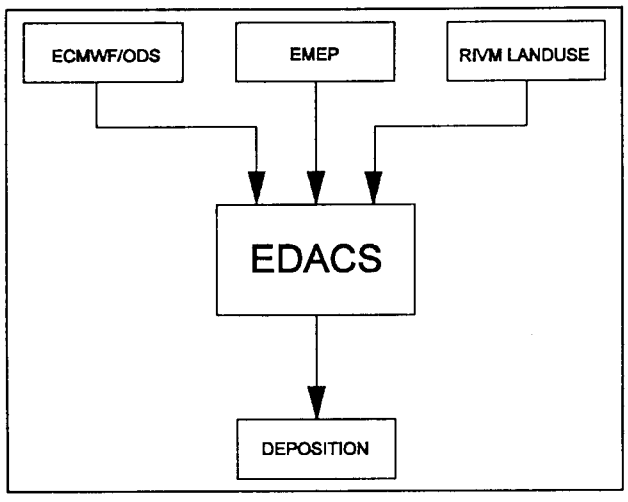

Fig A1 General outline of EDACS.

EDACS makes use of three main sources of data: the ECMWF/ODS meteorological observations, the EMEP-LRT in-air concentrations and the RIVM land-use data base. The spatial representation of the data are depicted in Figures A2-A3.
The RIVM Land-use data base (*rivmlu*) is an Arc/Info[1] pseudogrid coverage of 1/6°x1/6° lat/long gridcells. Each gridcell has a unique identity that is used as a key to access other data tables. The principal associated data table is *lu_grid*, with land-use attribute data for all gridcells. Arc/Info procedures outlined in Figure A4 have been used to add longitude and latitude coordinates to each gridcell and to subsequently export cell-identity, co-ordinates and lu_grid land-use attribute data to an ascii file *eurogridatt.exp*. A fortran program *exchange* uses this file, along with interpolated meteorological data and the dry deposition module *depac*, to calculate dry deposition data (*vdm* files) for SO_2,NO_2,NO,NH_3,HNO_3 and particles for 6-hour intervals. The dry deposition parameterizations are deduced for a limited number of surface types. To couple the parameterizations to a certain land-use data base a conversion

[1] The GIS system used is Arc/Info version 6.

between land-use classifications has to be made. In Table A1 the land-use types used in EDACS and its conversions are presented. The land-use types in the first column of Table A1 are used to estimate the minimal stomatal resistance of vegetation. The latter column is used to define the soil and in-crop resistance.

The meteorological data is extracted from the ECMWF Observational Data Set for a given time-period and a given area with a fortran program *ecmwfselect*. The program *ecmwfsurface* interpolates a number of meteorological parameters to a 0.5°x1.0° lat-long grid.

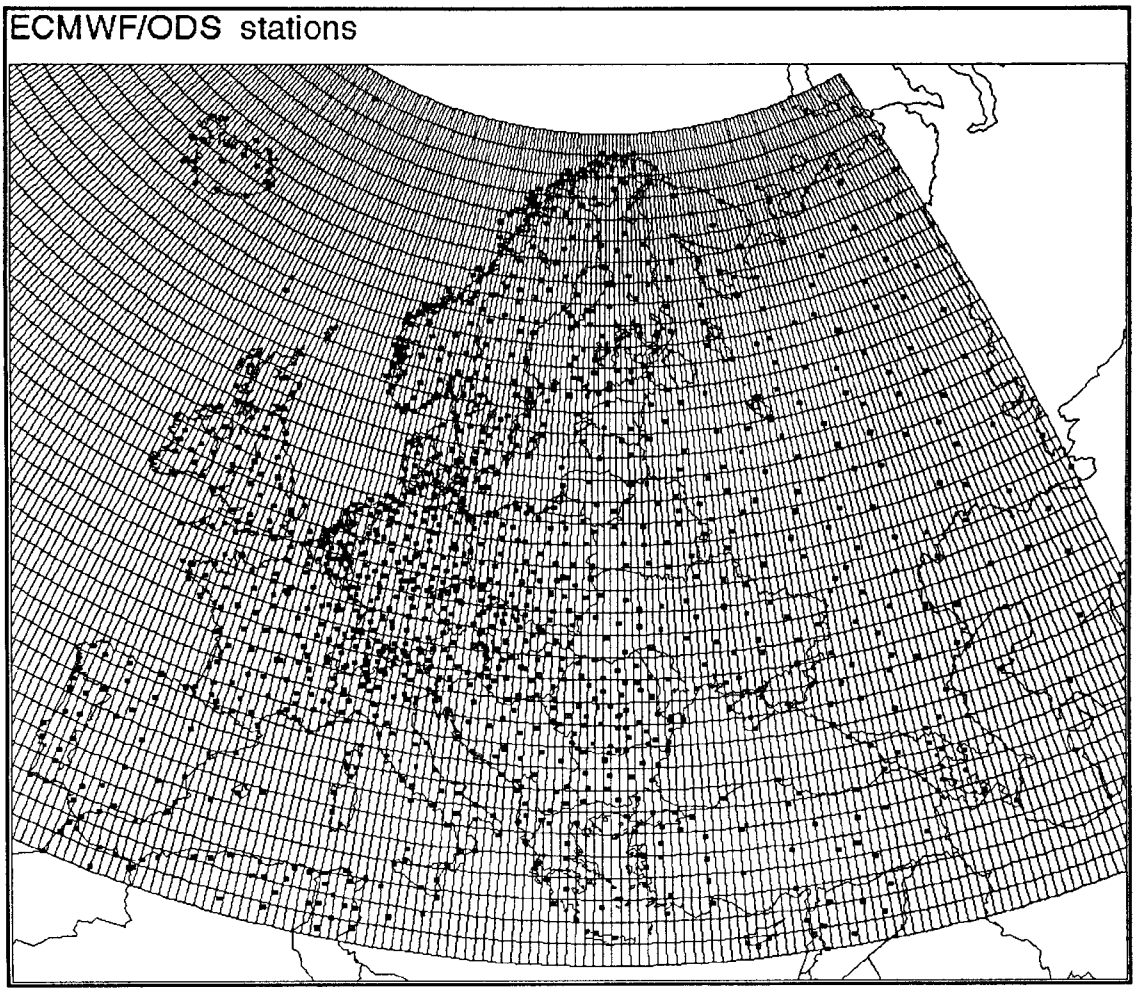

Figure A2 The position of the selected meteorological stations of the ECMWF Observational Data Set. The 0.5°x1.0° grid used in the ***ecmwfsurface*** *interpolation program is also shown.*

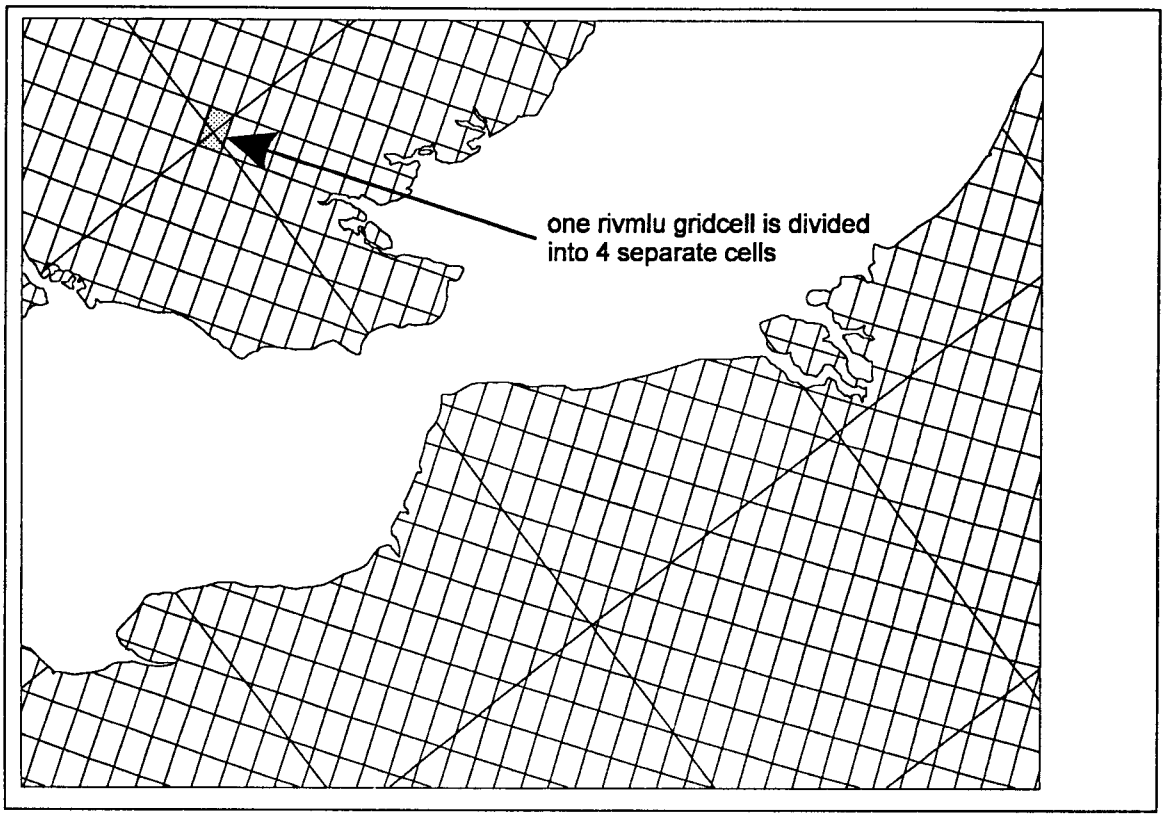

Fig A3 A part of the RIVM/LBG land-use grid on 1/6°x1/6° lat/long scale and the EMEP-LRT grid on a 150x150km scale. An intersection of the land-use grid with the EMEP grid is indicated. Each rivmlu gridcell may be covered by 1,2,3 or 4 EMEP gridcells.

Table A1 RIVM Land-use types and conversions

Land-use type according to		
Wesely (1989)	RIVM/LBG	EDACS (1994)
agricultural land	grassland or arable land	grassland
agricultural land	arable	cultivation
agricultural land	permanent crops	cultivation
coniferous forest	forest	coniferous forest
water (salt and fresh)	inland water	water
urban land	urban area	urban

Accumulated deposition is calculated by the *drycalcdepo* procedure. This fortran program uses as input:
1) daily vdm files (as calculated by *exchange*)
2) daily emep files (extracted from emep data base)

In the procedure the fortran program *calcindexes* uses examples of a vdm and emep file and the euroemeclnok.exp file to calculate for each record in euroemepclnok.exp indexes of corresponding records in the vdm and emep file. The index file is then used as an input to calcdepo as well as daily files for vdm and emep air concentrations for the specific period. This speeds up the calculation of accumulated daily deposition values considerably.

The deposition data is calculated for each polygon that results from an intersection of the *rivmlu* grid and the EMEP grid (Figure A3). This intersection coverage (*euroemepclnok*) is cleaned up and exported to an ascii file *euroemepclnok.exp* that *drycalcdepo* uses as lookup table. Accumulated dry deposition is then written to an output file that is read back into an Arc/Info database table.
The accumulated wet deposition for 1989 is calculated from the EMEP data base by *ladmireaddepo*, the resulting data is read into an Arc/Info database table.
Total deposition is then calculated by addition of dry and wet deposition results for each intersected polygon in *euroemepclnok,* using an Arc/Info calculation procedure.
Arc/Info arcplot is then used to produce maps of total deposition.

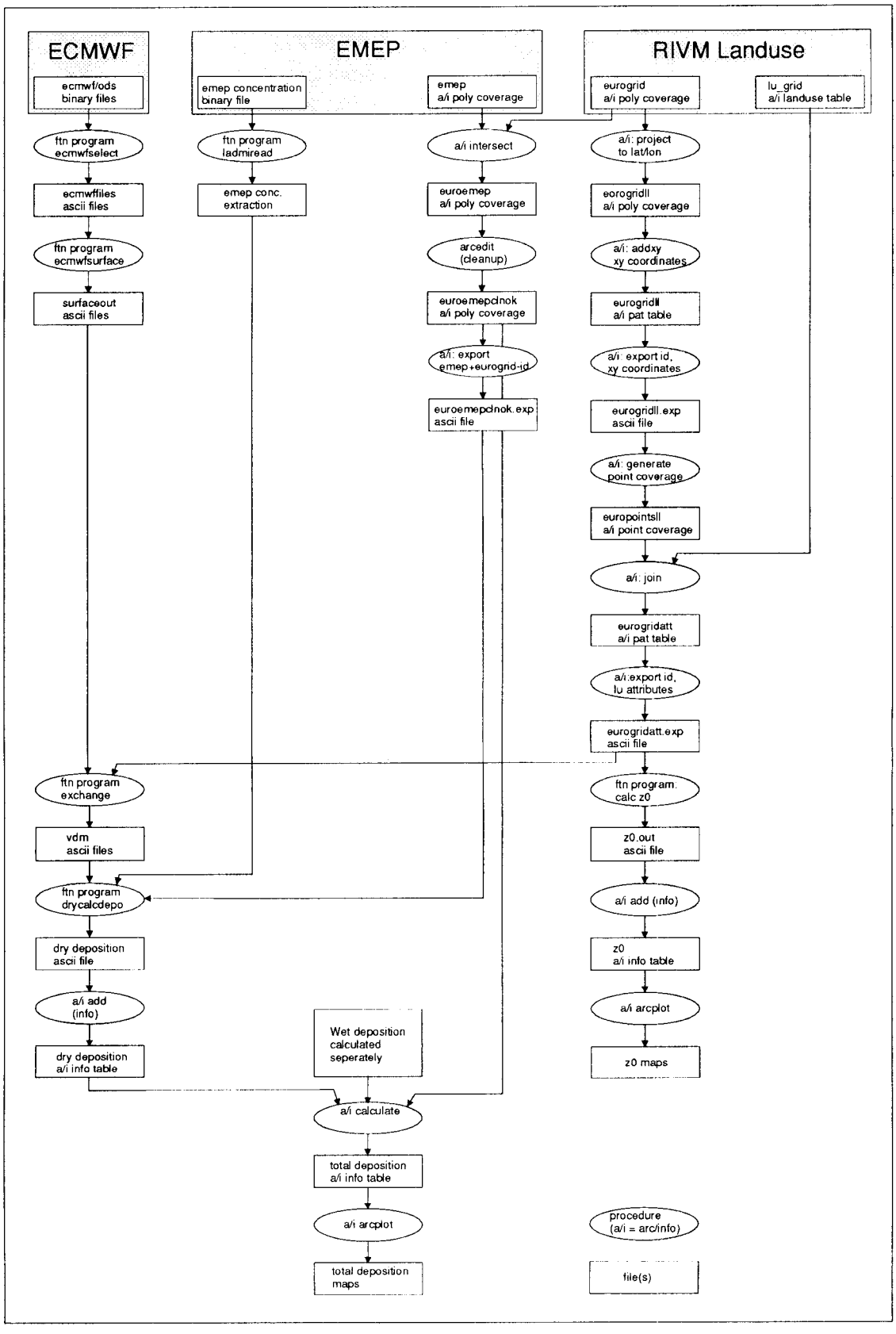

Fig A4 Flow chart of the ArcInfo procedures (drycalcdepo).

Appendix B Description of the deposition module DEPAC

The parameterizations of the deposition velocity V_d for each component are described here. This is a summary of the paper by Erisman *et al.* 1994. This paper is based on previous publications among others Wesely (1989), Lövblad *et al.* (1993) and recent dry deposition measurements e.g. carried out in the EUROTRAC/BIATEX program. Only the parameterizations used in the DEPAC fortran code will be given. For a discussion on the choices of the parameterizations the reader is referred to the above paper and references therein.

For NH_3 and NO, bi-directional fluxes can occur. With the module DEPAC it is possible to distinguish between deposition and emission of the components (see Table B4). However, emissions are not taken into account in the present EDACS version and in DEPAC the surface conductance in those cases is set at zero.

The r_{urban} for urban area is not given in Erisman *et al.*, 1994. The r_{urban} is set at 1000 s m^{-1} under dry surface conditions for all components. This is for SO_2 and NO_x based on Walcek *et al.*, 1986 and Voldner *et al.*, 1986.

The deposition velocity V_d is the inverse of three resistances:

$$V_d(z-d) = \frac{1}{r_a(z-d) + r_b + r_s} \qquad \text{(B1)}$$

The three resistances represent the three stages of transport, the aerodynamic resistance r_a for the turbulent layer, the laminar layer resistance r_b for the quasi-laminar layer, and the surface or canopy resistance r_s for the receptor itself. Below the parameterizations of these resistances will be presented.

Aerodynamic resistance r_a

The atmospheric resistance to transport of gases across the constant flux layer is assumed to be similar to that of heat (e.g. Hicks *et al.*, 1989). r_a is calculated with:

$$r_a(z-d) = \frac{1}{\kappa u_*}\left[\ln\left(\frac{z-d}{z_0}\right) - \psi_h\left(\frac{z-d}{L}\right) + \psi_h\left(\frac{z_0}{L}\right)\right] \qquad \text{(B2)}$$

in which κ is the Von Karman constant (0.4), u_* is the friction velocity, L is the Monin Obukhov length and z_0 is the roughness length. $\psi_h[(z-d)/L]$ is the integrated stability function for heat. The atmospheric resistance to transport of gases across the constant flux layer is assumed to be similar to that of heat (e.g. Hicks *et al.*, 1989). u_* and L are calculated using

procedures described in Beljaars and Holtslag (1990).

Quasi-laminary boundary layer resistance r_b

The quasi-laminar layer resistance r_b is approximated by the procedure presented by Hicks *et al.* (1987):

$$r_b = \frac{2}{\kappa u_*}\left(\frac{Sc}{Pr}\right)^{2/3} \qquad \text{(B3)}$$

where *Sc* and *Pr* are the Schmidt and Prandtl number respectively. *Pr* is 0.72 and *Sc* is defined as: $Sc = \upsilon/D_i$, with υ being the kinematic viscosity of air (0.15 $cm^2\ s^{-1}$) and D_i the molecular diffusivity of pollutant *i*. The Schmidt and Prandtl number correction in Equation B3 is listed in Table B1 for different gases.

Table B1. Schmidt and Prandtl number correction in Equation B3 for different gaseous species and the diffusion coefficient ratio of water to the pollutant *i*.

Component	D_{H2O}/D_i	$(Sc/Pr)^{2/3}$
SO_2	1.9	1.34
NO	1.5	1.14
NO_2	1.6	1.19
NH_3	1.0	0.87
HNO_3	1.9	1.34
H_2O	1.0	0.87

Surface resistance r_s

The surface resistance of gases consists of other resistances, either determined by the actual state of the receptor, or by a memory effect. r_s is a function of the canopy stomatal resistance r_{stom} and mesophyll resistance r_m; the canopy cuticle or external leaf resistance r_{ext}; the soil resistance r_{soil} and in-canopy aerodynamic resistance r_{inc}, and the resistance to surface waters r_{wat} (Equation B4). In turn, these resistances are affected by leaf area, stomatal physiology, soil and external leaf surface pH, and presence and chemistry of liquid drops and films. The

stomatal resistance, external leaf surface resistance and soil resistance act in parallel:

$$r_s = \left[(r_m + r_{stom})^{-1} + (r_{inc} + r_{soil})^{-1} + r_{ext}^{-1}\right]^{-1} \quad \text{(B4)}$$

water surface: $r_s = r_{wat}$
bare soil: $r_s = r_{soil}$
snow covered surface: $r_s = r_{snow}$

In the following sections the parameterizations of the different resistances for different gases will be given.

Stomatal resistance r_{stom}

The stomatal resistance for water vapour, r_{stom}, is described with a parameterization given by Wesely (1989) which is based on a method by Baldocchi *et al.* (1987) and only needs data for global radiation Q (W m^{-2}) and surface temperature T_s (°C):

$$r_{stom} = r_i \{1 + [\frac{200}{Q + 0.1}]^2\} \{\frac{400}{T_s(40 - T_s)}\} \quad \text{(B5)}$$

Values for r_i can be obtained from a look-up table for different land-use categories and seasons as listed in Table B2 (taken from Wesely, 1989). This general framework for the water vapour stomatal resistance can be used to describe stomatal uptake for each gas by correcting the r_{stom} using the ratio of the diffusion coefficient of the gas involved to that of water (Table 1) and adding the mesophyll resistance:

$$r_{stom,i} = r_{stom} \frac{D_{H_2O}}{D_i} + r_m \quad \text{(B6)}$$

The mesophyll resistances for all the gases are assumed to be zero, because of insufficient knowledge (Voldner *et al.*, 1986 and Wesely, 1989).

In-canopy aerodynamic resistance r_{inc}

Deposition to canopies includes vegetation and soil. A substantial amount of material can be deposited to the soil below the vegetation. The in-canopy aerodynamic resistance r_{inc} for vegetation is modelled with (van Pul and Jacobs, 1994):

$$r_{inc} = \frac{b\,LAI\,h}{u_*} \qquad \text{(B7)}$$

where LAI is the one sided leaf area index, h the vegetation height, b an empirical constant taken as 14 m^{-1}. In winter, when deciduous trees are leafless, LAI is set at 1. In this way the exchange caused by penetration of gusts is accounted for in a very straightforward way.

Table B2. Internal resistance r_i (s m^{-1}) to be used for estimating the stomatal resistance for different seasons and land-use types using Equation (B5). Entities of 9999 indicate that there is no air-surface exchange via that resistance pathway (adopted from Wesely, 1989).

Land-use type / seasonal category	1	2	3	4	5	6	7	8	9	10	11
Midsummer with lush vegetation	9999	60	120	70	130	100	9999	9999	80	100	150
Autumn with unharvested cropland	9999	9999	9999	9999	250	500	9999	9999	9999	9999	9999
Late autumn after frost, no snow	9999	9999	9999	9999	250	500	9999	9999	9999	9999	9999
Winter, snow on ground and subfreezing	9999	9999	9999	9999	400	800	9999	9999	9999	9999	9999
Transitional spring with partially green short annuals	9999	120	240	140	250	190	9999	9999	160	200	300

(1) Urban land, (2) agricultural land, (3) range land, (4) deciduous forest, (5) coniferous forest, (6) mixed forest including wetland, (7) water, both salt and fresh, (8) barren land, mostly desert, (9) non forested wetland, (10) mixed agricultural and range land, and (11) rocky open areas with low-growing shrubs.

Surface resistance for SO_2

The deposition of SO_2 on vegetation has been shown to be regulated mainly by stomatal resistance and the presence of surface water on the foliage. SO_2 dry deposition is enhanced over wet surfaces. However, an understanding of the variations of surface resistance with

surface wetness chemistry is limited. It is assumed here that when the surface is wet, deposition of SO_2 is regulated by external leaf uptake. Erisman et al (1993) derived a r_{ext} parameterization for wet surfaces (due to precipitation and an increase in relative humidity) of heather plants (in s m^{-1}):

during or just after precipitation: $r_{ext}=1$,
in all other cases:

$$\begin{aligned} r_{ext} &= 25000\exp[-0.0693\,rh] \qquad rh<81.3\% \\ r_{ext} &= 0.58\,10^{12}\exp[-0.278\,rh] \qquad rh>81.3\% \end{aligned} \tag{B8}$$

where rh is the relative humidity (in %). Equation B8 is assumed to be valid for all vegetated surfaces in Europe. Equation B8 is applied to air temperatures above -1 °C. Below this temperature it is assumed that surface uptake decreases and r_{ext} is set at 200 s m^{-1} (-1 < T < -5°C) or 500 s m^{-1} (T < -5°C). The soil resistance, r_{soil} is set at 500 s m^{-1}. For snow covered surfaces:

$$\begin{aligned} r_{snow} &= 500 \qquad T<-1^oC \\ r_{snow} &= 70(2-T) \qquad -1<T<1^oC \end{aligned} \tag{B9}$$

The surface resistance for water, r_{wat}, is set at 50 s m^{-1}.

Surface resistance for NH_3

NH_3 is emitted from fertilised soils and from pasture during grazing. In addition, emission takes place from crops, ungrazed pasture and semi-natural vegetation under dry, warm conditions during daytime at low ambient concentrations. In other cases NH_3 is mainly deposited. Deposition in these cases is regulated by stomatal uptake and by deposition to external leaf surfaces. The external leaf resistance is parameterized via a look-up table, see Table B3. Essentially these are observed net r_c values taking into account the cuticle resistance and emission under dry and wet conditions and for *managed vegetation* and *semi-natural (unfertilised) ecosystems and forests.* In this table, conditions where emission is expected are marked.
The soil resistance, r_{soil} is set at 100 s m^{-1}. For snow covered surfaces equation B9 is used. The surface resistance for water and soil or vegetation wetted by precipitation or dew is set at 10 s m^{-1}.

Table B3. Net-r_c for NH_3 (s m^{-1}) over different managed vegetation categories in Europe. Winter conditions: T> -1 °C, otherwise r_s=200 s m^{-1} (-1 < T < -5 °C) or r_c=500 s m^{-1} (T<-5°C).

Land-use category	Day		Night	
	Dry	Wet	Dry	Wet
Pasture during grazing:				
summer:	1000#	1000#	1000	1000
winter:	50	20	100	20
Crops and ungrazed pasture:				
summer:	r_{stom} #	50	200	50
winter:	r_{stom} #	100	300	100
Semi-natural ecosystems and forests	500#	0	1000	0

#:emission estimated as $F_{em}=-c(z)/(r_a+r_b+r_s)$, at ambient ammonia concentrations below 2 μg m^{-3}

Surface resistance for NO_2

Deposition of NO_2 is mainly regulated by stomata. The deposition to external leaf surfaces, water surfaces and soils is one order of magnitude smaller.
The external resistance here equivalent to the cuticle resistance is set at 2000 s m^{-1}. The surface resistance for water and soil or vegetation wet by precepitation or dew is set at 2000 s m^{-1}. Also for snow the surface resistance is set at 2000 s m^{-1}.

Surface resistance for NO

For NO at ambient concentrations, emission from soils is observed more frequently than deposition. This emission, the result of microbial activity in the soil, is dependent on soil temperature, water content and ambient concentrations of NO (Hicks *et al.*, 1989). It has been observed from grassland, agricultural land and forest soils. The external resistance here equivalent to the cuticle resistance is set at 10000 s m^{-1}. The surface resistance for soil and for soil and vegetation wet by precepitation or dew is set at -1000 s m^{-1}. With the latter effectively emission is indicated (see Table B5).

Surface resistance for HNO_3

Deposition of HNO_3 seems to be limited by the aerodynamic resistance only. For these gases the external surface resistance is found to be negligible: r_{ext} is set at 10 s m^{-1} for calculation reasons. At low temperatures, T < -5 °C, with a snow covered surface the r_{ext} is set at 50 s m^{-1}.

r_{soil}, r_{snow} and r_{wat} values for the above gases are summarised in Table 5.

Table B5. Surface resistance values (s m^{-1}) for soil surfaces r_{soil}, snow covered surfaces r_{snow} and water surfaces r_{wat}.

Gas	Soil surfaces r_{soil}		Water surfaces r_{wat}	Soil or water pH	Snow covered surfaces r_{snow}	Temperature (°C)
	Wet	Dry				
SO_2	0 500	1000 Eq. B8	0 500	>4 <4	70(2-T) 500	-1<T<1 T<-1
NH_3	250 0	500# 50#	500 0	>8 <8	70(2-T) 500	-1<T<1 T<-1
NO	1000#	1000#	2000	-	2000	-
NO_2	2000	1000	2000	-	2000	-
HNO_3	0	0	0	>2	0 100	T>-5 T<-5

#:emission estimated as $F_{em}=-c(z)/(r_a+r_b+r_s)$

Parameterization of particle deposition

The resistance analogy is not used for particles. For sub-micron particles, the transport through the boundary layer is more or less the same as for gases. However, transport of particles through the quasi-laminar layer can differ. For particles with a diameter < 0.1 μm, deposition is controlled by diffusion, whereas deposition of particles with a diameter > 10 μm is more controlled by sedimentation. Deposition of particles with a diameter between 0.1 and 1 μm is determined by the rates of impaction and interception and depends heavily on the

turbulence intensity. Deposition velocity for particles with a diameter in this range can be obtained from parameterizations in terms of L and u_*, according to Wesely *et al.* (1985):

$$V_d = \frac{u_*}{a} \qquad L>0$$
$$V_d = \frac{u_*}{a}\left[1+\left(\frac{300}{-L}\right)^{2/3}\right] \qquad L<0 \tag{B10}$$

where a=500 for low vegetation. For forest a=100 according to Erisman (1992).